Research Article **Open Access**

Keith Attenborough*, Imran Bashir, and Shahram Taherzadeh

Exploiting ground effects for surface transport noise abatement

DOI 10.1515/noise-2016-0001
Received Sep 29, 2015; accepted Feb 11, 2016

Abstract: Growing demand on transportation, road and railway networks has increased the risk of annoyance from these sources and the need to optimise noise mitigation. The potential traffic noise reduction arising from use of acoustically-soft surfaces and artificial roughness (0.3 m high or less) is explored through laboratory experiments, outdoor measurements at short and medium ranges and predictions. Although the applicability of ground treatments depends on the space usable for the noise abatement and the receiver position, replacing acoustically-hard ground by acoustically-soft ground without or with crops and introducing artificial roughness configurations could achieve noise reduction along surface transport corridors without breaking line of sight between source and receiver, thereby proving useful alternatives to noise barriers. A particularly successful roughness design has the form of a square lattice which is found to offer a similar insertion loss to regularly-spaced parallel wall arrays of the same height but twice the width. The lattice design has less dependence on azimuthal source-receiver angle than parallel wall configurations.

Keywords: soft ground effect; insertion loss; transport noise; parallel walls; lattice

1 Introduction

Ground effects are the result of interaction between direct sound travelling from source to receiver and sound from source to receiver that is reflected at the ground. The interaction includes both destructive interference or cancellation and constructive interference or reinforcement. Over smooth acoustically-hard ground, the frequencies at which cancellations and reinforcements occur depend only on the difference between the lengths of the ground-reflected and direct path. The size of this difference depends only on source and receiver heights and the distance separating source and receiver positions. For road/tyre noise sources and a 1.5 m high receiver separated by 20 m or more of hard ground, the destructive interferences are at too high frequency for there to be much influence on the spectrum so the presence of hard ground leads more or less to doubling of sound pressure compared with no ground. On the other hand for an engine noise at 0.3 m and a 4 m high receiver at 20 m distance, the destructive interferences due to hard ground occur in a frequency range of importance. Nevertheless, in practice complicating factors such as multiple sources, atmospheric turbulence and naturally uneven and non-uniform ground mean that the actual increases in traffic noise level due to hard ground corresponds more nearly to energy doubling [1].

Most naturally-occurring outdoor surfaces are porous and as a result sound is able to penetrate the porous surface. Ground-reflected sound is thereby subject to a change in phase as well as having some of its energy converted into heat. This results in a complex ground impedance, defined as the ratio of sound pressure to (the normal component of particle) velocity at the surface, and, not only is the magnitude of sound reduced on reflection, but also the phase change due to the finite (complex) ground impedance combines with the phase change due to path length difference. This has the consequence that, for a given source-receiver geometry, the first destructive interference occurs at a lower frequency than over hard ground and leads to the well-known reduction in outdoor noise levels, often called ground attenuation, that features in many prediction schemes and has been studied extensively [2]. Even if the ground is flat, alongside typical surface transport corridors the ground impedance varies with range. The influence of impedance discontinuities has also been studied and is incorporated to some extent in prediction schemes.

According to ISO 9613-2 [1], any ground surface of low porosity is 'acoustically-hard', *i.e.* perfectly sound-

***Corresponding Author: Keith Attenborough:** Engineering and Innovation, The Open University, Milton Keynes, MK7 6AA, UK; Email: keith.attenborough@open.ac.uk
Imran Bashir: Department of Renewable Energy, University of Exeter, Cornwall Campus, TR10 9EZ, UK
Shahram Taherzadeh: Engineering and Innovation, The Open University, Milton Keynes, MK7 6AA, UK

reflecting, and any grass-, tree-, or potentially vegetation-covered ground is 'acoustically-soft', *i.e.* perfectly sound-absorbing. Although this might be an adequate representation in some circumstances, it oversimplifies the considerable range of properties and resulting effects.

According to the common methodological framework for strategic noise mapping under the Environmental Noise Directive (2002/49/EC) [3], "the acoustic absorption properties of ground are mainly linked to its porosity". While porosity is important for one kind of "soft" ground effect (the other kind being due to roughness and is discussed later in this Section and in Section 5), the acoustical properties of porous ground are affected most by the ease with which air can move in and out of the ground surface. This is indicated by the *flow resistivity* which represents the ratio of the applied pressure gradient to the induced steady volume flow rate of air through the surface of the ground. The porosity of naturally-occurring ground surfaces does not vary as much as their flow resistivity. If the ground surface has a high flow resistivity, it means that it is difficult for air to flow through the surface. This can result from very low or negligible surface porosity. Hot-rolled asphalt and non-porous concrete have near zero porosity and a very high flow resistivity whereas many forest floors and freshly-fallen snow have very much lower flow resistivity and a high porosity.

The method in the EC Directive [3], is similar to ISO9613-2 [1] in that it allows for frequency-dependent ground effect over non-flat ground by defining equivalent heights and using a dimensionless frequency independent coefficient G that takes values between 0 (acoustically-hard) and 1 (acoustically soft) according to the type of ground [3]. In ISO9613-2 the mean value of G along a path indicates the fraction of the path that includes porous ground. In a similar manner to HARMONOISE and NORD2000 [4, 5], the EU Directive 2015/996 scheme [3] identifies types of ground corresponding to various flow resistivity values (see Table 1). However eight flow resistivity classes are associated with only four different values of the G factor. Various forms of grass-covered ground are featured in the descriptions of types C, D and E. Ground type E which includes "compacted lawns" is assigned a G factor of 0.7 whereas types C and D, including "turf", "grass" and "pasture" are given a G factor of 1.0. As discussed later, "grassland" involves an even wider range of ground effects.

Also, particularly if the ground is otherwise acoustically-hard, roughness, even at scales smaller than the shortest wavelength of interest, affects outdoor sound propagation. Essentially the presence of small-scale roughness makes a surface that appears acoustically-hard at normal incidence appear acoustically-soft at near grazing angles, The influence of roughness on ground effects has not been studied extensively and, so far, there is no explicit allowance for ground roughness in prediction schemes.

Although prediction schemes allow for ground effect, none of them suggest ways of exploiting ground effects for noise control. Possible ground treatments explored in this paper include (i) replacing acoustically-hard ground by acoustically-softer ground in a single strip or in multiple strips or patches, (ii) choosing the soft surface that achieves greatest attenuation, augmenting its contribution with vegetation, and (iii) deliberate roughening of hard ground.

2 Measurements

We report unpublished results of two types of measurements investigating ground effects since they add to those published elsewhere by the authors and by others. We have made laboratory measurements of excess attenuation (EA) spectra *i.e.* spectra of the attenuation in excess of that due to wave front spreading. This required a measurement of the free field spectrum (in the absence of the surface) for the same geometry. EA spectra have been obtained from measurements in a 4.3 m × 4.3 m × 4.3 m anechoic chamber (designed to be anechoic above a frequency of 125 Hz). A Maximum Length Sequence System Analysis (MLSSA) was used for signal generation and signal processing. Essentially the MLSSA output represents an impulse response. The MLS signal has a flat frequency response over a broad frequency range and gives a high signal to noise ratio. Inside the anechoic chamber, the level of ambient noise is very low, and it is found that a MLS sequence of order 16 offers a reasonable compromise between measurement time and good signal to noise ratio. A point source consisting of a Tannoy driver fitted with a 0.02 m internal diameter 1.0 m long brass tube, was used for laboratory measurements. While capable of producing good signal up to 20 kHz, the source emitted little sound energy below 300 Hz. In the laboratory, quarter-inch ACO-pacific type microphones were used as receivers.

Also we have made outdoor measurements of the spectra of the difference between the sound level spectra measured by two vertically or horizontally separated microphones at a certain height above the ground surface. The level difference (LD) represents a transfer function between two microphones and is independent of the source spectrum. Since the outdoor environment involves a de-

Table 1: Categories of ground and associated *G* values in the Directive 2015/996 prediction scheme [3].

Description	Type	Flow resistivity kPa s m^{-2}	*G* value
Very soft (snow or moss like)	A	12.5	1
Soft forest floor (short, dense heather-like or thick moss)	B	31.5	1
Uncompacted, loose ground (turf, grass, loose soil)	C	80	1
Normal uncompacted ground (forest floor, pasture field)	D	200	1
Compacted field and gravel (compacted lawns, park area)	E	500	0.7
Compacted dense ground (gravel road, parking lot)	F	2000	0.3
Hard surfaces (most normal asphalt, concrete)	G	20000	0
Very hard and dense surfaces (dense asphalt, concrete, water)	H	200000	0

gree of turbulence, a continuous broadband noise source was used instead of an MLS signal. Measurements were repeated several times and averaged to improve the signal to noise. Low frequency wind noise was avoided by high pass filtering during post-processing. A B&K type 4295 point source, specially designed as a point source for audio-frequency measurements between 80 Hz and 10 kHz, was used for outdoor measurements. Two B&K type 4189-B-001-½ inch microphones were used for level difference measurements. A laptop installed with Matlab and data acquisition tool box connected to 16 bit National Instruments-USB 6259 data acquisition box (NI-DAQ) together with a Matlab code was used for controlling the outdoor measurement system. The code is capable of generating a digital signal, communicating and controlling the NI-DAQ, acquiring the measured input and storing it in a digital form. The code also offered the capability to do a quick on-site analysis.

3 Ground impedance models and data

The acoustical properties of ground surfaces may be represented by the surface impedance defined as the ratio of incident sound pressure at the surface to the associated air particle velocity at right angles to the surface. Because of phase changes at the surface due to viscous and thermal effects in the pores this impedance is represented as a complex quantity with real and imaginary components. The ground surface may be considered as that of a rigid-framed porous material and there are many models for the impedance of rigid-porous materials that involve one or more parameters including flow resistivity. Theories for propagation from a point source over an finite impedance ground require impedance data or models for impedance spectra. Ground impedance can be deduced from complex pressure ratios measured at short ranges in an impedance-model-independent way. But since it is difficult to make accurate measurements of phase outdoors, to date relatively few deductions of ground impedance from complex pressure ratio measurements have been reported [7]. It is more common to deduce parameter values for impedance models by fitting short range level difference magnitude spectra using "template" methods [7, 8]. Subsequently these models and parameter values can be employed in prediction schemes.

A one parameter semi-empirical model [9], the single parameter being flow resistivity, has been used widely for outdoor sound prediction. The frequency-dependent ground effects predicted by the EU Directive 2015/996 method [3] with G factors of 1, 0.7 and 0.3 correspond closely to those predicted using this one parameter model with the flow resistivity values listed for ground types D, E and F in Table 1.

A comparison of the applicability of many of these models [10], based on fitting data obtained at short range using signals from a point source at vertically-separated microphones in connection with the ANSI [7] and NORDTEST [8] standards, has shown that, for many grasslands, two parameter models lead to better agreement with data than the semi-empirical one parameter model. Moreover it is pointed out in detail elsewhere [10–12] that it is not advisable to use single parameter semi-empirical models for representing ground impedance since (a) they are not physically admissible (for example at low frequencies they lead to predictions of negative real parts of the surface impedance and complex density), (b) they do not perform as well in fitting short range propagation data as other physically admissible impedance models and (c) that a result of the different frequency dependence of impedance spectra they predict, if used to predict long range ground effect spectra, they yield predic-

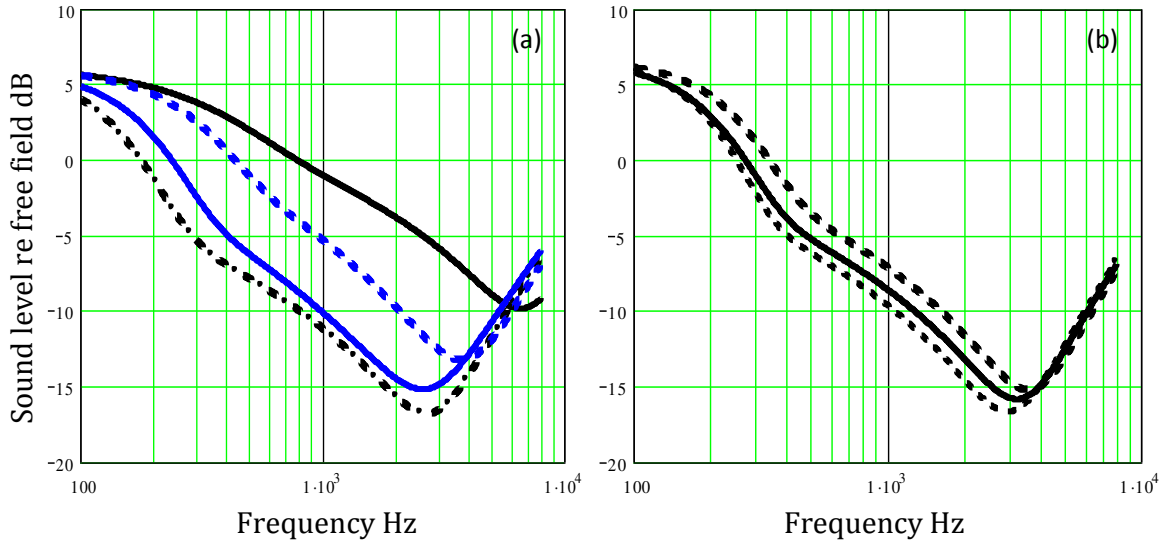

Figure 1: (a) Predictions of the potential variation in excess attenuation spectra with source height 0.05 m, receiver height 4 m and horizontal separation 100 m over "grassland" with highest and lowest impedance spectra represented by the 2-parameter variable porosity model (solid and dot-dash black lines respectively see Table 2) and by the Delany and Bazley single parameter empirical model for categories D and E in Table 1 (broken and solid blue lines respectively) (b) predictions of the seasonal variation in excess attenuation spectra over "lawn" for the same geometry using the 2-parameter variable porosity model parameters for mean (solid line), maximum and minimum (broken lines) impedance spectra. Moderate turbulence is assumed [2].

Table 2: Variable porosity model parameters giving best fits to short range level difference magnitude data obtained at five grassland locations [10, 12].

Grassland description	Flow resistivity kPa s m^{-2}	Effective depth m
Pasture NORDTEST site #26	824.6	0.07
Pasture NORDTEST site #19	383.4	0.09
long grass NORDTEST #20	167.2	0.08
Lawn NORDTEST site #1	75.3	0.09
Heath NORDTEST #44	51.9	0.12

tions that differ significantly from those resulting from use of physically admissible models that, in any case, give better fits to short range data.

Not surprisingly, the most common ground type for which data are available is "grassland". Table 2 lists values of effective flow resistivity and effective depth for several types of grassland obtained by using the physically admissible two-parameter variable porosity impedance model [2, 10, 13] to fit data for short range level difference magnitudes [10, 13]. The second parameter of the variable porosity model, other than effective flow resistivity, can be stated either as rate of change of porosity with depth (abbreviated later to porosity rate) or as effective depth. These interpretations are related by effective depth = 4/porosity rate. The flow resistivity values listed in Table 2 vary by a factor of more than sixteen compared with the factor of six variation in the (effective) flow resistivity values listed for grassland (categories C, D and E) in Table 1 (based on the single parameter Delany and Bazley impedance model [9]). Although, the lowest flow resistivity value for grass (80 kPa s m^{-2}) is listed for category C, categories C and D in Table 1 have the same G value thereby restricting the potential variation of ground effects due to grassland predicted by the EU Directive 2015/996 scheme [3]. Moreover, even though a value of 200 kPa s m^{-2} is listed for category D, the minimum flow resistivity that has been used in calculating the G factor is 300 kPa s m^{-2} [14].

There may be seasonal variations in "soft" ground effect due to changes in moisture content. Table 3 lists the best fit parameter values, using the variable porosity model, corresponding to short range level difference measurements made over a lawn during a study of spatial and seasonal variations [11, 15]. The parameters listed include the maximum and minimum effective flow resistivity values that fit the means of a series of measurements in "Summer" and "Winter" conditions (corresponding to dry and wet) [11]. Figure 1(a) compares predictions of ex-

Table 3: Mean, maximum and minimum parameter values corresponding to fits to short range level difference spectra over lawn using the two-parameter variable porosity impedance model [11].

	Summer		Winter	
	flow resistivity kPa s m^{-2}	layer thickness m	flow resistivity kPa s m^{-2}	layer thickness m
mean	80	0.035	200	0.011
maximum	105	0.023	285	0.008
minimum	60	0.035	115	0.018

cess attenuation spectra in a moderately turbulent atmosphere [2] for (point) source height 0.05 m, receiver height 4 m and range 100 m using the two-parameter variable porosity model for the lowest and highest effective flow resistivity values listed in Table 2 and the single parameter empirical model with the flow resistivity values listed for ground categories D and E in Table 1. Figure 1(b) shows excess attenuation spectra for the same geometry and turbulence parameters for the maximum, minimum and mean parameter values listed in Table 3. The potential variation in excess attenuation over 100 m of grassland (Figure 1(a)) is in excess of that predicted using the Delany and Bazley impedance model with the effective flow resistivities in only categories D and E in the EU Directive 2015/996 scheme [3] and significantly exceeds the seasonal differences predicted for a particular grassland (Figure 1(b)).

The large differences in effective flow resistivity values for grassland lead to substantial differences in the corresponding predictions of ground effect at 1.5 m high receivers 50 m from a highway or at 4 m high receivers 125 m from a highway which will be presented in section 5d. To make such predictions it is necessary to allow for the discontinuity in impedance between the acoustically-hard road surface and the receiver over acoustically-soft ground. So ways of predicting the effects of impedance discontinuities are reviewed in the next sub-section.

4 Impedance discontinuities

4.1 Single discontinuity

When sound propagates close to a mixed impedance ground surface, it diffracts at each change in impedance. The models developed to predict such sound propagation fall into two major categories: numerical and semi-analytical. Robertson *et al.* [16] study sound propagation over a mixed impedance ground surface using semi-analytical parabolic equation approximations and found good agreement with data. A computationally intensive numerical method based on a boundary integral equation formulation [17] for calculating the sound propagation over a single or multiple impedance discontinuities is found to give very good agreement with data also. An efficient and accurate numerical method for determining the sound field over a plane containing a single discontinuity between impedances Z_1 and Z_2 considers a hypothetical planar source 40 wavelengths wide and 20 wavelengths tall placed above the discontinuity [18]. The planar source is discretized into an array of point sources a fifth of a wavelength apart. The relative strength of each source is calculated using classical point source theory for propagation over infinite impedance Z_1. The received field is calculated as the sum of the contributions from each of the constituent planar sources over an infinite Z_2. However, comparison between predictions of this relatively numerically-intensive method and the De Jong semi-empirical formula (discussed shortly), and comparisons with data indicated that the De Jong formula is adequate for engineering purposes.

Semi-empirical methods need less computational resources. Naghieh and Hayek [19] present an analytical solution to predict the sound propagation from a point source over a ground with single impedance discontinuity but this requires a numerical integration. The solution due to Enflo and Enflo [20] for sound propagation over an infinite plane with an impedance discontinuity, although involving simpler calculations, is only valid when the impedance discontinuity is many wavelengths from the source and the receiver. De Jong *et al.* [21] propose a widely used semi-empirical model for sound propagation over a single hard-to-soft impedance discontinuity with the discontinuity perpendicular to the direction from the source to receiver axis. The De Jong model uses semi-empirical modifications of analytical expressions for diffraction by a rigid half-plane. Daigle *el al.* [22] compare data from measurements over single impedance ground surface with the De Jong model predictions [21]. They show that the agreement between data and De Jong model predictions is good except when the source and receiver are placed

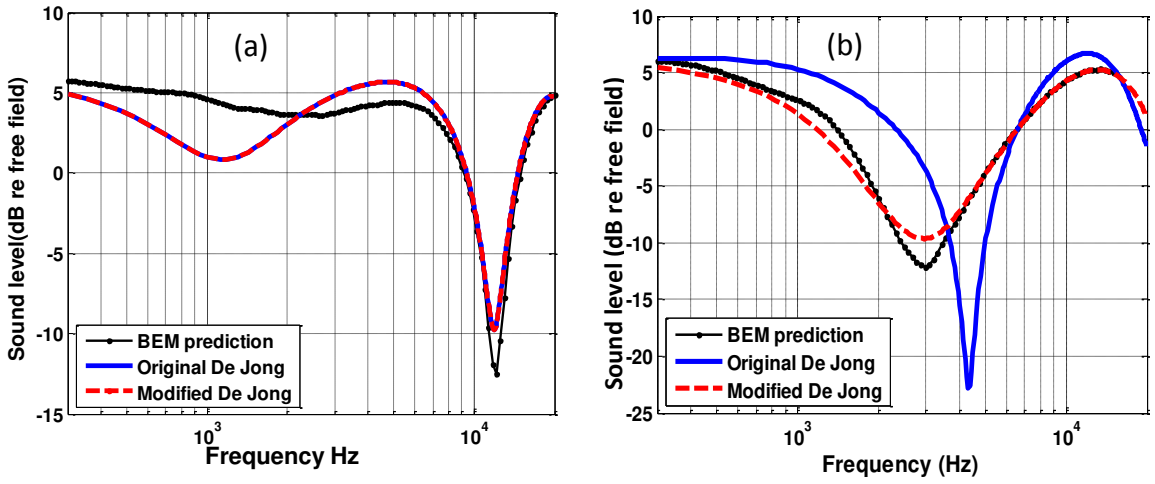

Figure 2: Comparison of BEM predictions with predictions of original and modified de Jong models for propagation between source and receiver at 0.07 m height separated by 0.7 m over an impedance discontinuity 0.6 m from the source between simulated MDF board (hard) and felt over MDF board (soft) (a) hard to soft and (b) soft to hard [25].

very close to the ground surface *i.e.* near grazing. Hothersall and Harriott [17] confirm that the De Jong method gives good agreement with data over single impedance discontinuity. They extend the single discontinuity De Jong model to encompass two discontinuities and obtained agreement with data and calculations using the boundary integral solution. They conclude that De Jong formulation for two impedance discontinuities only gives good agreement with the data for greater source and receiver heights and shorter source to receiver distances. This is similar to the limitation observed by Daigle *el al.* [22] for a single discontinuity. Boulanger *et al.* [23] show that De Jong model gives good agreement with laboratory data for propagation over a single impedance discontinuity; however it fails if there are multiple impedance discontinuities. Lam and Monazzam [24] observe that the De Jong semi-empirical model, derived initially for a hard-to-soft discontinuity (during propagation away from the source) fails to satisfy reciprocity and modified it accordingly. Their modification improves the agreement between data and De Jong type predictions for propagation from soft to hard ground. Numerical results obtained with the Boundary Element Method (BEM) have been used extensively as reference results to establish the accuracy of analytical or semi-analytical methods.

Figure 2(a) compares BEM and de Jong predictions for propagation over single hard to soft or soft to hard discontinuities [25]. The (point) source and receiver are assumed at 0.07 m height and separated by 0.7 m (typical of the laboratory geometries for which more data is presented subsequently). The high impedance surface is considered to be a medium density fibreboard (MDF) and the low impedance surface is a layer of felt on MDF. Both surfaces are characterised by the variable porosity impedance model [10] with effective flow resistivity values and porosity change rates of 30 kPa s m^{-2} and 15 m^{-1} and 100 MPa s m^{-2} and 15 m^{-1} for the soft and hard surfaces respectively. These comparisons confirm that the modification of the de Jong method by Lam and Monazzam [24] gives predictions that are closer to those made using BEM than the original de Jong formulation particularly for the soft to hard discontinuity.

4.2 Multiple discontinuities

Much previous work has focussed on a single impedance discontinuity. Much less attention has been given to multiple impedance discontinuities. Figure 3(a) shows an example laboratory measurement arrangement and Figure 3(b) compares resulting data for the excess attenuation spectra over various mixed impedance surfaces formed from rectangular strips of MDF and soft strips (felt, sand, lead shot) of equal widths (2.85 cm) and heights (1.2 cm) [25]. The felt and MDF used to make strips and patches were of the same thickness so that the resulting composite surfaces were plane.

Measurements are repeated for each source-receiver geometry after replacing the felt strips with sand or lead shot. Either an acoustically hard (MDF) strip or a soft (felt, sand or lead shot) strip is placed at the point of specular reflection which was halfway between source and receiver which were at equal heights. Strips are tightly packed to avoid gaps at the impedance discontinuities. Five mea-

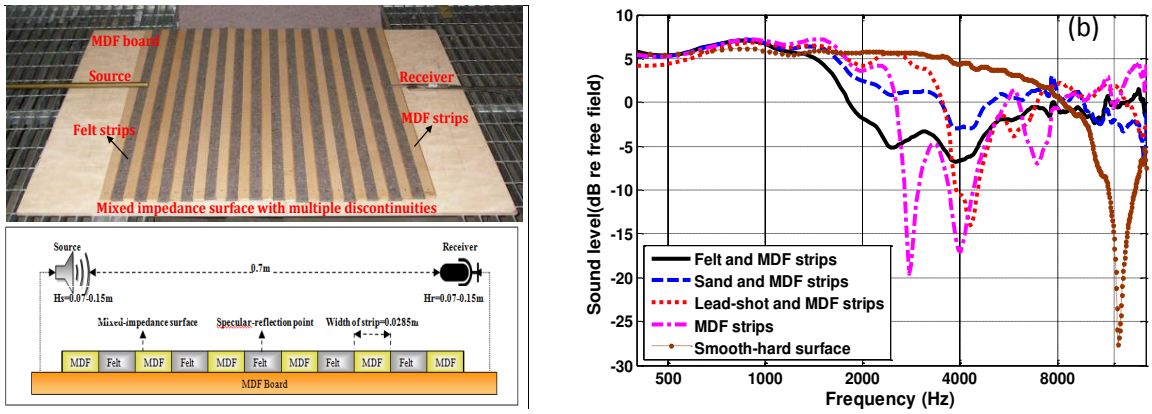

Figure 3: (a) An example measurement arrangement with strips of felt on MDF for investigating the effects of multiple impedance discontinuities in the laboratory (b) Example Excess Attenuation spectra measured with (point) source and receiver at 0.05 m height separated by 0.7 m over surfaces consisting of (i) felt and MDF strips (black solid line), (ii) sand and MDF strips (blue dash line), (iii) lead-shot and MDF strips (red dotted line) and (iv) MDF strips with centre-to-spacing of 0.057 m (magenta dash-dotted line) placed on MDF board. The measured EA spectrum for the smooth hard surface (brown dotted line) is shown also [26].

surements are carried out over each surface but with different source and receiver heights for each measurement.

Also shown in Fig. 3(b) is the EA spectrum measured for the same source-receiver geometry over the smooth MDF board. In comparison to those for the smooth hard surface, the EA maxima are at lower frequencies for both mixed impedance and rough hard surfaces. Hard rough surfaces produce multiple distinct and sharp EA maxima. While these are present to some extent in the EA spectra obtained over mixed impedance surfaces, they are broader and their magnitudes are less. The depths of EA minima (attenuation maxima) depend on the impedance contrast. EA measurements over felt and sand have shown that felt is acoustically "softer" than sand or a thin layer of lead shot. Hence, the EA maxima obtained over felt and MDF strips are deeper than the EA maxima observed over sand and MDF strips. EA spectra for rough hard surfaces will be discussed further in section 5c.

Another semi-analytical approach for predicting sound propagation over mixed impedance ground is the Fresnel-zone method proposed by Hothersall and Harriott [17]. It is the simplest of the available methods and can be applied to either a single impedance discontinuity or to multiple impedance discontinuities since it does not distinguish between them. It assumes that the reflecting area in a discontinuous plane is related simply to the region around the specular reflection point defined by a Fresnel-zone condition. A Fresnel zone method is used to account for discontinuous terrain in the HARMONOISE prediction scheme [4]. Boulanger *et al.* [23] propose a modification to the Fresnel zone scheme used by Hothersall and Harriot [17]. Instead of the linear interpolation of two excess attenuations, Boulanger *et al.* [23] use a linear interpolation between the two pressure terms. This modified Fresnel-zone method gives better agreement with data. Figure 4(a) compares EA spectra measured with source and receiver at a height of 0.12 m and at a horizontal separation of 0.7 m over surface composed of felt and MDF strips with modified Fresnel-zone predictions. The Fresnel-zone method predicts only approximate EA spectra which ignore diffraction at the impedance discontinuities so the agreement between data and predictions is not very good. This confirms that the Fresnel-zone approximation, while potentially satisfactory for predicting overall broadband levels, is not useful for detailed predictions over multiple discontinuities. Figure 4(b) compares BEM predictions with the same laboratory data. Although the detailed agreement between BEM predictions and data is not particularly good, the overall agreement with these data is better than obtained with the Fresnel zone method.

Figure 5(a) shows a "chequerboard" arrangement of felt and MDF squares. Figure 5(b) compares EA spectra measured with source and receiver at 0.07 m height and 0.7 m separation over both the 'strip' and 'chequerboard' arrangements of felt and MDF [25]. The EA spectra in Figure 5(b), obtained with the source-receiver axis normal to the mixed impedance area *i.e.* normal to the strips, are more or less similar which suggest that there is little advantage in using 3D distributions of patches rather than 2D strips for the configuration in which the source-receiver axis is normal to the array. However data obtained with the source-receiver axis at a series of azimuthal angles (see Figure 6) show that propagation over the 3D "chequer-

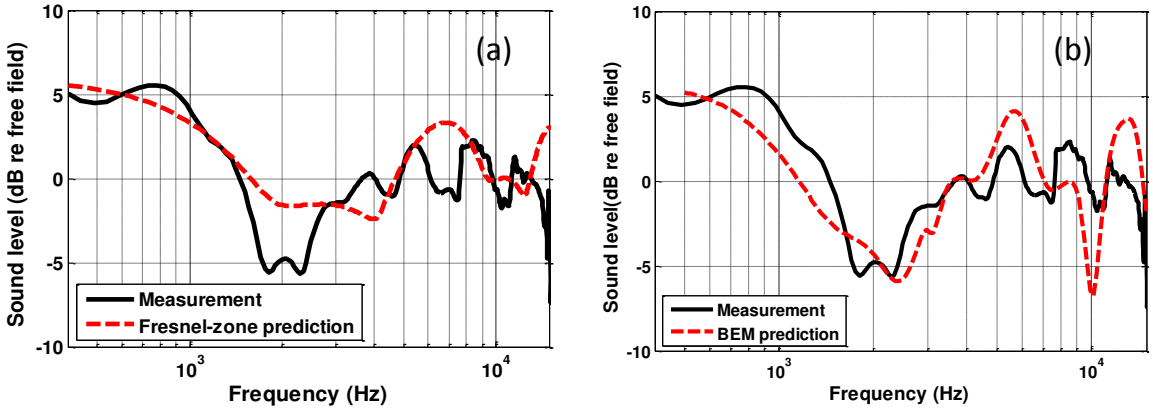

Figure 4: Comparison between excess attenuation spectra measured with source and receiver at 0.12 m height separated by 0.7 m over surface consisting of felt and MDF strips and predictions using (a) the modified Fresnel zone method [23] and (b) BEM.

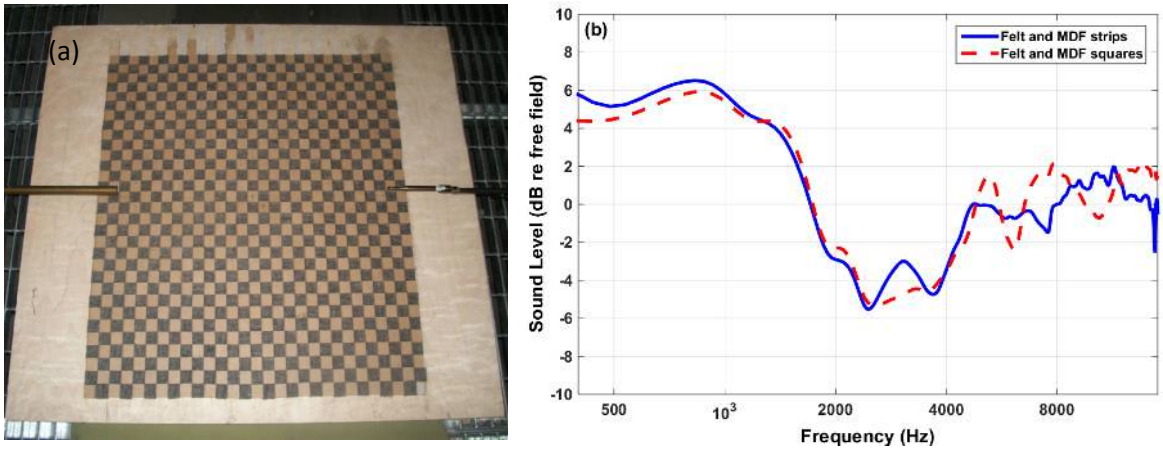

Figure 5: (a) A "chequerboard" surface of felt and MDF squares (b) EA spectra measured over the 'chequerboard' and 'strip arrangements with source and receiver at 0.07 m heights and separated by 0.7 m [25].

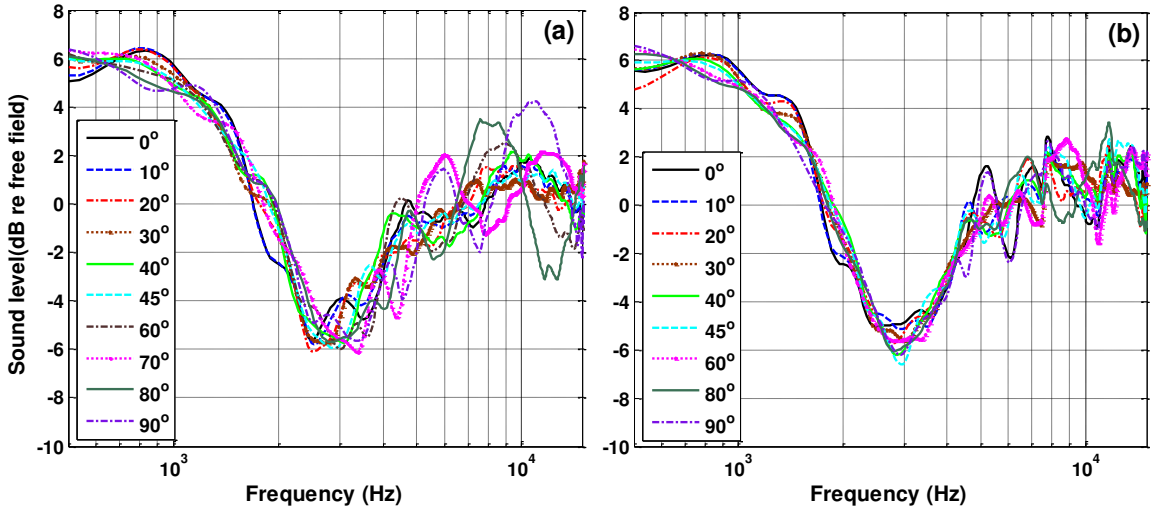

Figure 6: EA spectra measured at different azimuthal angles over (a) Felt and MDF impedance strips and (b) Felt and MDF patches. The measurements were carried out by placing source and receiver at a height of 0.07 m and a separation of 0.7 m above the surface.

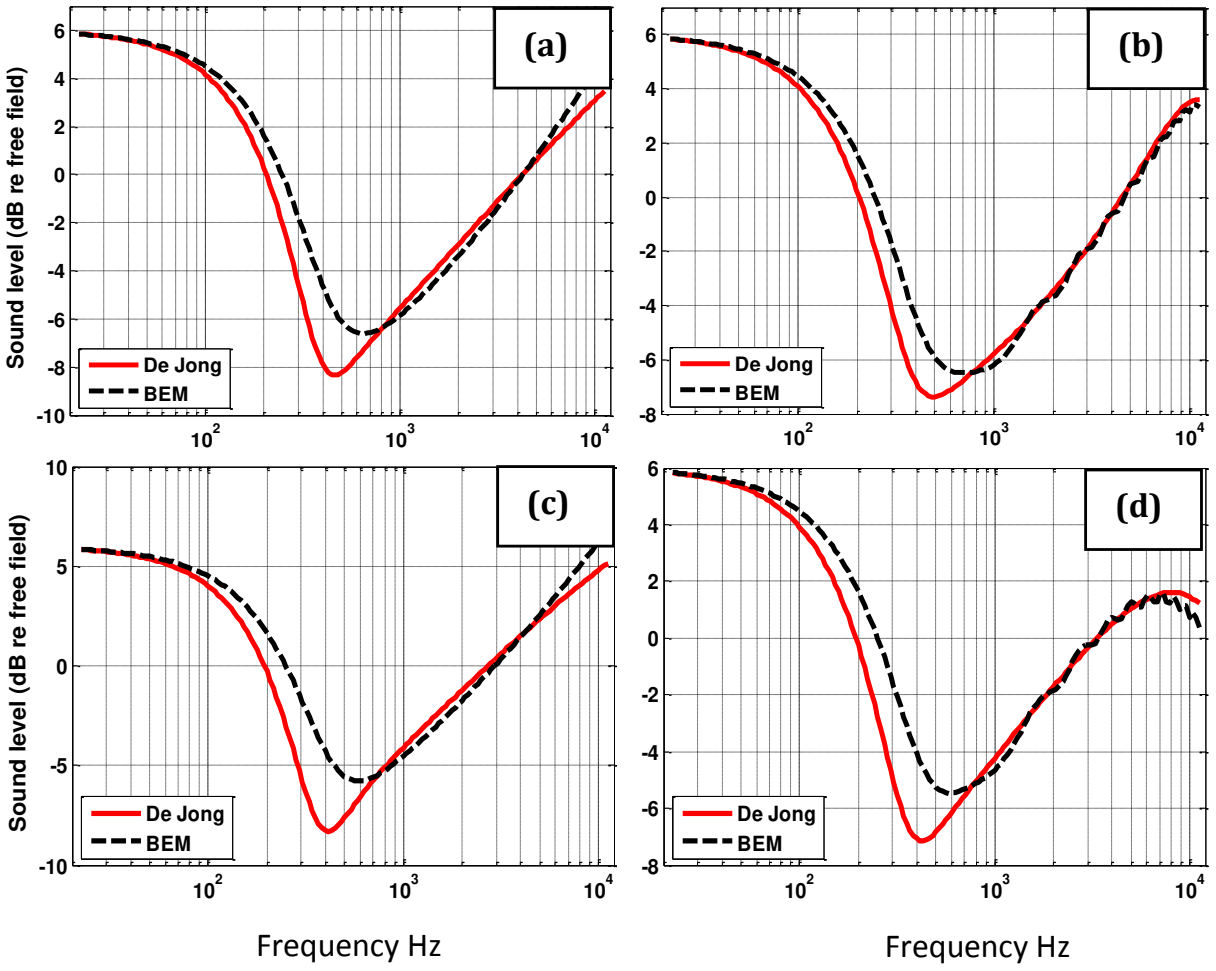

Figure 7: Comparison between EA spectra predicted by the De Jong model [21] and BEM for a single hard/soft impedance discontinuity at a distance of 5.0 m from the source over hard ground [25]. The soft ground impedance after the discontinuity is calculated using the 2-parameter slit pore model [10] (Flow resistivity = 104 kPam^{-2}, Porosity = 0.36 similar to "long grass" in Table 2). The source-receiver geometry with source height (Hs) receiver height (Hr) and range (R) is (a) Hs = 0.01 m, Hr = 1.5 m, r = 50 m (b) Hs = 0.3 m, Hr = 1.5 m, r = 50 m (c) Hs = 0.01 m, Hr = 1.5 m, r = 53.5 m (d) Hs = 0.3 m, Hr = 1.5 m, r = 53.5 m.

board" arrangement has less dependence on azimuthal angle.

4.3 Impedance discontinuity models for traffic noise computations

Although BEM enables reasonably good predictions for propagation over mixed impedance ground surface at laboratory scales, it is computationally expensive when used for the larger scale geometries that will be of interest in section 5d. Since the modified De Jong semi-empirical model is a much less computationally-intensive alternative to BEM it is interesting to explore its accuracy. Figure 7 compares its predictions with BEM predictions for a particular ground type and four geometries typical of those considered in section 5d.

The agreement between de Jong and BEM predictions of propagation over a single discontinuity is good for higher source and receiver heights [25]. Consequently the de Jong model has been used for single impedance discontinuity situations in the calculations reported in section 5d. However, as exemplified in Fig. 8, predictions of the modified de Jong and Fresnel zone models for propagation over a double impedance discontinuity, corresponding to a single 10 m wide strip of soft ground starting 2.5 m from the source, do not agree with BEM predictions [25]. Consequently, unless stated otherwise, BEM has been used for the multiple impedance calculations reported in section 5d.

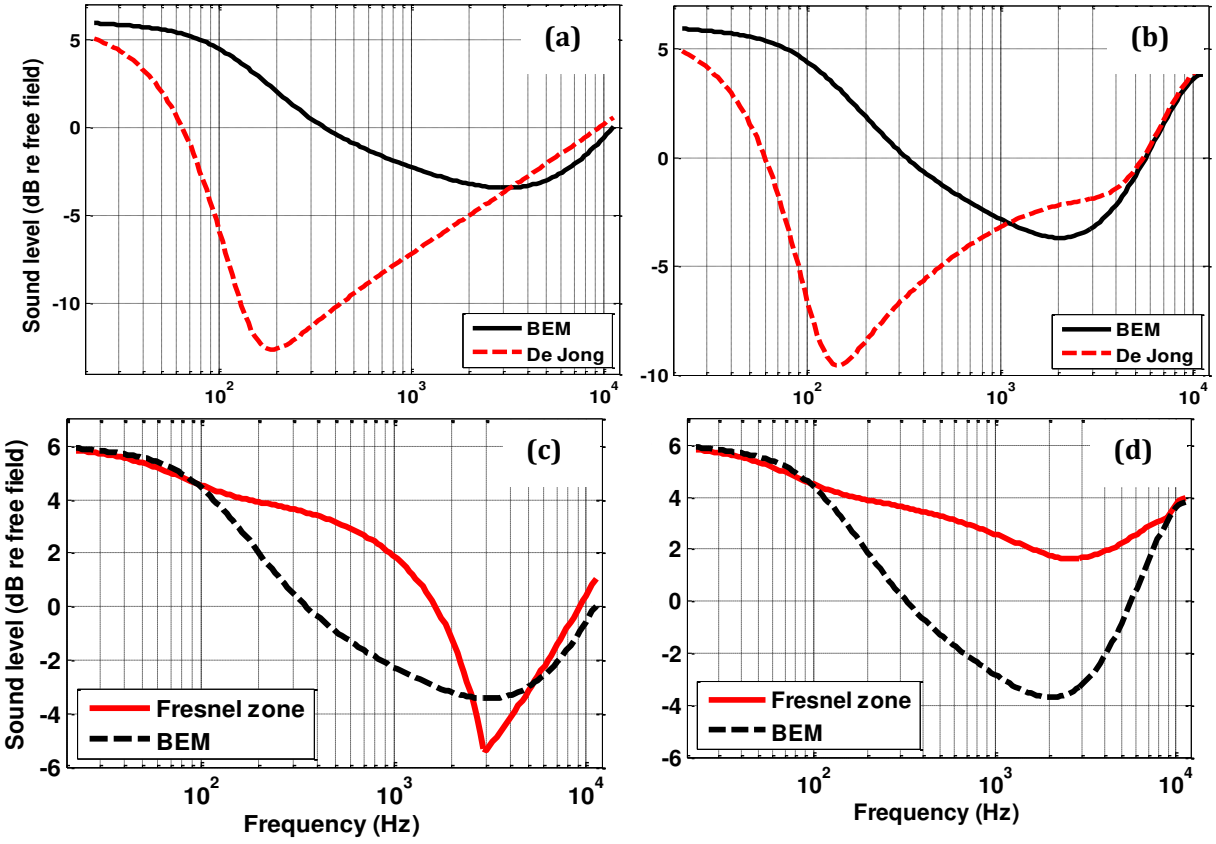

Figure 8: EA spectra [25] predicted by De Jong and Fresnel zone models [17, 21] and BEM for propagation over a 10 m wide "soft" strip with impedance given by the 2-parameter slit pore model [10] with flow resistivity of 10 kPa s m^{-2} and a porosity of 0.4, the distance between the source and receiver was assumed to be 50 m (a) and (c) source height 0.01 m, receiver height 1.5 m (b) and (d) source height 0.3 m, receiver height 1.5 m.

4.4 Extra attenuation due to crops

When plants grow in porous ground their roots create root zones which change the near-surface flow resistivity and porosity. Hence the presence of plants results in a different ground effect to that for the same ground with little or no vegetation. The best fit impedance model parameters obtained from short range vertical level difference measurements over ground containing winter wheat crops [25] are an effective flow resistivity of 170 kPa s m^{-2} and a porosity of 0.2 using the two parameter slit pore model [10]. These values can be compared with those obtained over nearby bare ground, *i.e.* the same type of soil but on which no crops were growing or had been grown [25]. The best fit flow resistivity and porosity values over the bare unplanted ground are 2000 kPa s m^{-2} and 0.2 respectively which suggests that growing winter wheat reduced the effective flow resistivity of the soil surface by at least a factor of 10.

Foliage and stems in vegetation scatter sound and sound energy is converted into heat by viscous and thermal processes at leaf surfaces. In trees and bushes there will be scattering by trunks and branches also. As a result of measuring sound transmission loss through dense corn, hemlock, red pine trees, hardwood brush and dense reeds in water, Aylor [26 (a) and (b)] has suggested that there is a relationship between a normalised excess attenuation, *i.e.* the attenuation in excess of that due to ground effect divided by the square root of the product of foliage area per unit volume and the scattering parameter (which is the product of wave-number and a characteristic leaf dimension). On the basis of these suggestions, the data in Figure 10, 11 are fitted empirically by [27]

$$\frac{EA(dB)}{\sqrt{FL}} = A\left[1 - \exp\left(0.3 - 0.5(ka)\right)\right], \quad ka \geq 0.6 \qquad (1)$$

where $EA(dB)$ represents the excess attenuation in dB, F/m is the foliage area per unit volume, L m is the length of the propagation path, k is the wavenumber = $2\pi f/c$, c being the adiabatic sound speed in air and a m is the mean leaf width. A is a constant with a value of 3 for best fit to

Aylor's data. The lower limit on ka avoids negative values of EA.

Through a series of measurements carried over winter wheat, rape seed and willow crops [25], horizontal level difference data are used to study the sound propagation through crops. Sound attenuation by crops occurs due to multiple scattering between the stems and leaves, loss of coherence and viscous and thermal losses due to foliage. However, the major contribution to attenuation due to crops is due to viscous and thermal losses, which can be predicted by using an empirical formula (see Eq. (1)). This may be termed the "crops effect".

At lower frequencies ground effect is dominant and there is little or no crops effect. At higher frequencies above 3–4 kHz the crops effect is dominant. It was also found that the ground and crops effects can be treated independently and can be added to obtain the total effect [27]. Green leaf crops result in more attenuation than dry crops with fallen leaves. Although the attenuation due to crops involves viscous and thermal losses, multiple scattering effects and loss of coherence, it is possible to avoid calculating the multiple scattering and loss of coherence effects and yet to obtain reasonable predictions by only adding ground effect to attenuation due to viscous and thermal losses using larger "effective" values for foliage per unit area and mean leaf size [27].

5 Ground roughening

5.1 2D roughness

If a surface is artificially or naturally rough, incident sound is not reflected perfectly but is scattered by the roughness. The distribution of the scattered sound depends on the roughness topology, the ratio of the roughness dimensions to the incident wavelength and the relative locations of source and receiver [2]. As long as a sufficient fraction of the reflected sound retains a phase relationship with the incident sound (*i.e.* there is significant coherent scattering and specular reflection) there can be a significant change in ground effect. Many laboratory experiments show that the influence of small scale roughness on propagation over hard and soft surfaces can be considered in terms of effective surface impedance [2, 28–32]. Also, particularly if the surface is acoustically-hard, roughness induces a surface wave. Tolstoy [33, 34] predicts "boundary waves" due to energy trapped between the roughness elements and formulates models for scattering from arrays of 2D strip elements with identical dimensions and shapes on a plane surface. However these do not include incoherent scatter and predict that the effective impedance of a rough hard surface is purely imaginary. A model of Lucas and Twersky [35] for scattering from a plane containing parallel semi-cylinders includes incoherent scatter and results in a non-zero real part of the effective surface impedance.

When a surface is curved (convex) and rough and source and receiver are near the surface, the roughness enhances the creeping wave at low frequencies but, as is the case over flat rough surfaces, increases attenuation at high frequencies [36].

One method of deliberately introducing roughness outdoors is to construct an array of low parallel walls. As long as the height of the walls is 0.3 m, which is approximately the wavelength of sound in air at 1 kHz, or less, they can be considered as a form of artificial ground roughness. The potential usefulness of regularly-spaced low parallel walls for road traffic noise reduction was suggested and demonstrated by outdoor experiments in 1982 [37]. An array of sixteen 0.21 m high parallel brick walls with edge-to-edge spacings of about 20 cm placed on compacted grassland was found to give a broadband (between 100 Hz and 12,500 Hz) insertion loss (IL) of slightly more than 4 dB(A) including insertion losses of up to 20 dB(A) in the 1/3 octave bands between 400 and 1000 Hz. The creation and subsequent attenuation of surface waves was considered as the main mechanism for noise reduction. Although surface wave creation is one of the consequences of placing a low parallel wall array on an acoustically-hard ground, as discussed later, the array has a significant influence on ground effect over a wider range of frequencies than those affected directly by the surface wave generation.

5.2 Diffraction-assisted rough hard ground effect

Bougdah *et al.* [38] report laboratory measurements over arrays of up to 17 thin walls with (equal) heights and spacing between 8 cm and 25 cm. They find a maximum overall insertion loss of 10.3 dB for a 3.25 m wide 14-wall array with height and spacing of 0.25 m with the wall nearest the source located at the specular reflection point halfway between source and receiver which were at 0.4 m height and separated by 10 m. They discuss three physical effects other than surface wave creation and the effective ground impedance that may be involved. One of these is quarter wave resonance. In an array of identical 0.3 m high walls, this resonance should occur at 283 Hz. Predictions and data discussed later show that this mechanism is not important. They refer also to diffraction-grating effects.

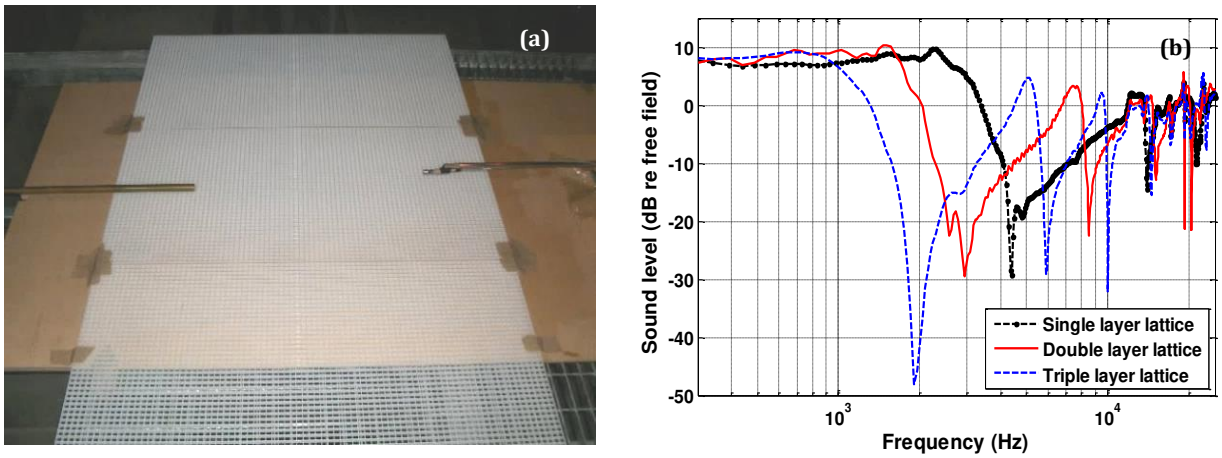

Figure 9: (a) Three adjacent sheets of a lighting diffuser lattice in the laboratory (b) EA spectra measured with source and receiver at 0.03 m height and 0.7 m separation over single, double and triple layers of the lighting lattice.

Essentially these are related to the diffraction-assisted ground effect, explored subsequently in more detail [39]. The third additional mechanism they suggest is that of interference between direct and multiply-reflected paths between adjacent walls. But this mechanism should be regarded as part of diffraction assisted ground effect rather than as a separate phenomenon.

More extensive laboratory measurements show that excess attenuation spectra are influenced by the number and spacing (edge-to-edge distance and regularity) of roughness elements and by their profile or shape [39]. These factors are not investigated by Bougdah *et al.* [38] who consider only regularly-spaced identical, thin acoustically-hard rib-like elements (vertical rectangular strips).

Comparisons of averaged excess attenuation spectra measured over various shapes of roughness elements in the laboratory [25, 39] show that random spacing of roughness elements leads to a broad and relatively shallow ground effect dip whereas up to three distinctive narrower attenuation maxima are observed if the identical roughness elements are distributed periodically. The first EA maximum may be regarded as roughness-induced ground effect. The frequencies of the second EA maximum depend on the spacing and the appearance of a third EA maximum depends on the percentage of ground surface 'exposed' between the roughness elements. Analysis shows that the first and third EA maxima observed over a periodically rough hard surface are frequency-shifted versions of the 1st and 2nd order smooth surface ground effect dips, whereas the second order EA maxima are diffraction grating related as a result of the periodic spacing of roughness elements.

Comparisons between laboratory experiments and predictions have shown that surfaces composed of closely-spaced parallel aluminium strips (width 0.0126 m, height 0.0253 m) placed with different edge-to-edge spacing between 0.003 m and 0.06 m on a hard surface (MDF) may be regarded as porous layers with vertical slit-like pores until their spacing approaches about 50% of the layer depth *i.e.* the strip height [39]. At larger separations they behave as periodically-rough surfaces. A heuristic effective impedance model for a periodically-rough surface is obtained by adding a modified Tolstoy imaginary roughness-induced impedance component to the impedance of a lossy hard-backed layer [39].

5.3 Propagation over lattices

A type of surface that creates an audio-frequency surface wave near grazing incidence is that formed by a plastic lighting diffuser lattice on a hard surface [25, 40–42]. Figure 8(a) shows three adjacent single thickness sheets of such a lattice on MDF and Fig. 8(b) shows EA spectra measured with source and receiver at a height of 0.03 m and separated by 0.7 m over single, double and triple lattice layers [25]. A single square cross section cell in the lattice has a side of 1.404 cm and is 1.263 cm deep. The lattice walls are 0.185 cm thick and the centre-to-centre spacing of the cells is 1.589 cm.

Over a single sheet of the lattice, most of the energy in the surface wave (indicated by EA magnitudes > 6 dB) is near 2 kHz. The main surface wave energy content and the first excess attenuation maxima are moved to higher frequencies as the layer depth is increased. Figure 10 shows data and predictions using a slit pore layer impedance

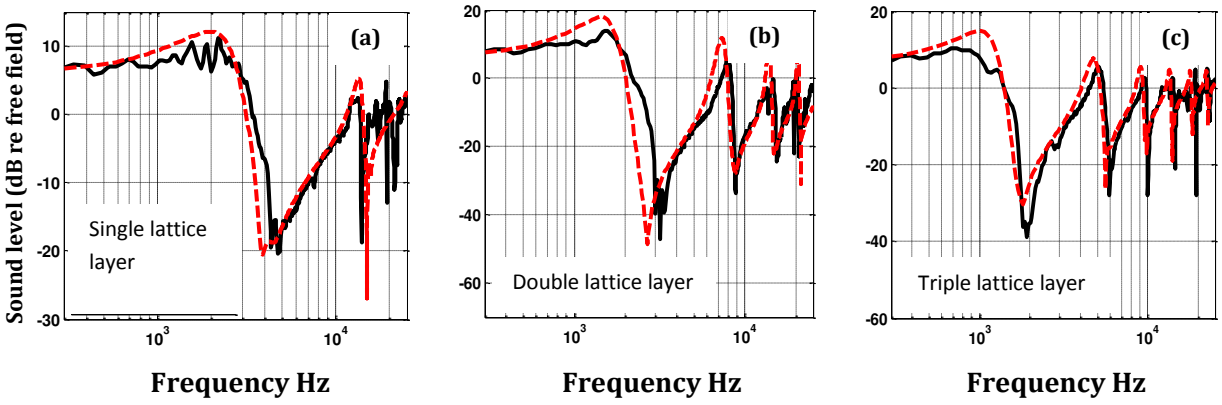

Figure 10: Measured and predicted excess attenuation spectra over (a) single, (b) double and (c) triple lighting lattice layers placed over MDF board with source and receiver at a height of 0.03 m and separated by 0.7 m. Predictions are for the field due to a point source over slit pore layer impedance with flow resistivity (3.35 Pa s m^{-2}), porosity (0.78) calculated from the lighting lattice cell dimensions and thickness equal to the relevant multiple of the lighting lattice thickness (0.01263 m).

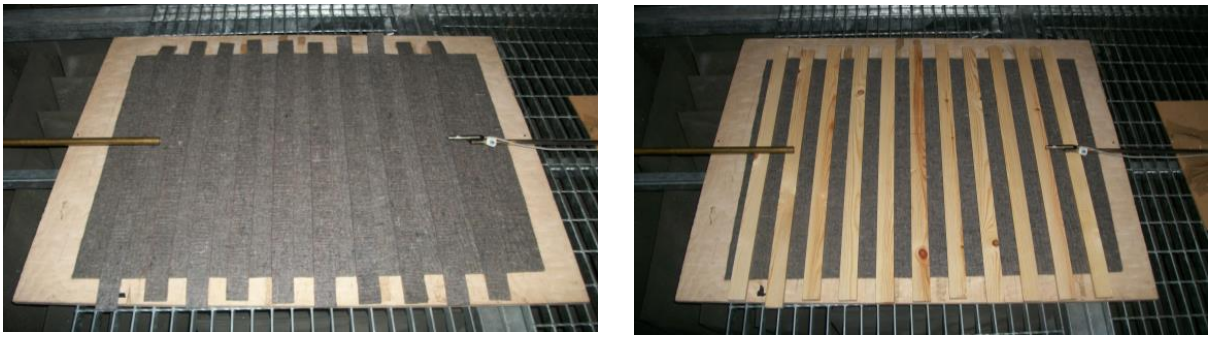

Figure 11: Two example laboratory arrangements for studying the effects of surface roughness: felt strips on a felt layer (left) and wooden strips on a felt layer (right) [25].

model [10] for source and receiver at a height of 0.03 m and separated by 0.7 m over single, double and triple lattice layers. The flow resistivity (R_s = 3.35 Pa s m^{-2}) and porosity (Ω = 0.78) of the slit pore layer are calculated from the lattice cell dimensions and the formula [2]:

$$R_s = \frac{2\mu T s_0}{\Omega r_h^2} \tag{2}$$

where μ is the dynamic viscosity coefficient in air, T is tortuosity, s_0 is a shape factor and r_h is the hydraulic radius. For the laboratory lattice the tortuosity is 1, the shape factor s_0 is 0.89 for and the hydraulic radius is equal to the cell width divided by 4 for square cells, which is 0.0035. The potential for using lattices for noise reduction is explored in sections 5.4 and 5.5. But since all of the smooth surfaces to which roughness is added considered so far have been acoustically-hard first we look at data and predictions for acoustically-soft surfaces that are roughened.

5.4 Acoustically-soft rough surfaces

5.4.1 Laboratory data on 2D rough surfaces

There is considerable laboratory data showing that the effect of adding small scale roughness to a surface, whatever its original impedance, is to modify its apparent impedance [2, 28–32]. If the original smooth surface is acoustically-hard then the effective impedance of the roughened surface is finite. If a surface is acoustically soft then the influence of roughening is to make the effective surface impedance less than the original surface impedance mainly through a reduction in its real part.

Figure 11 shows two example measurement arrangements in the laboratory and Figure 12 shows excess attenuation spectra measured over several model rough and smooth surfaces [25]. The reference acoustically-hard surface is MDF. The reference acoustically soft surface is a 0.012 m thick layer of felt. 0.045 m wide and 0.012 m thick

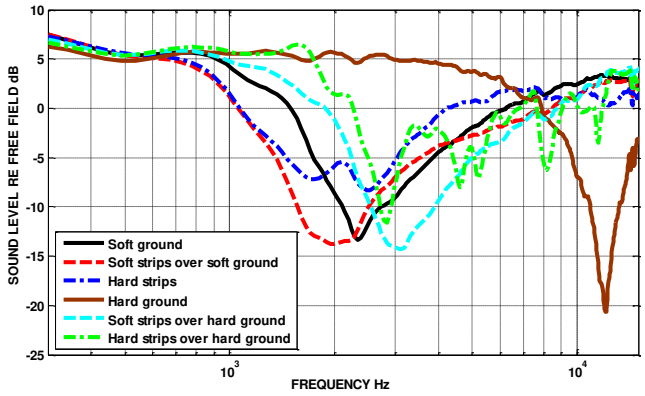

Figure 12: Laboratory data for excess attenuation obtained with (point) source and receiver at 0.07 m height and 0.7 m separation over various forms of rough surface ([25] see text).

strips of felt and wood were placed on either the felt layer or the MDF.

The data shown in Figure 12 are obtained with (point) source and receiver at 0.07 m height and separated by 0.7 m. The curves correspond to (i) the "hard ground" MDF surface showing a first EA maximum near 11 kHz, (ii) felt strips on MDF (soft strips over hard ground) with an EA maximum near 3 kHz, (iii) wooden strips on MDF (hard strips over hard ground) with the roughness-induced EA maximum just below 3 kHz and several higher frequency diffraction-grating-related maxima, (iv) the acoustically-soft felt surface (soft ground) with an EA maximum near 2.4 kHz (v) felt strips on felt (soft strips over soft ground) which gives a deep EA maximum centred around 2 kHz and (vi) wooden strips on felt (hard strips) resulting a shallow EA maximum below 2 kHz and another shallow EA maximum just above 2 kHz. The influence of any kind of roughness on the hard surface is noticeably greater than that of the same kind of roughness on the acoustically-soft surface.

5.4.2 Outdoor data for roughness effects on acoustically-soft ground

Measurements made outdoors over ground that has been recently cultivated *i.e.* ploughed or disked, [2, 25, 26, 43] show that the ground effect is changed. In accordance with laboratory data [29] an increase in surface roughness results in a decrease in the real part of the effective impedance. When the original surface is soil, there may also be a decrease in the surface flow resistivity as the result of the cultivation. Figure 13 shows that excess attenuation spectra measured before and after disking [26] can be fitted by using a two-parameter impedance model [10]. After disking, the fitted effective flow resistivity is less, as indicated by the lower frequency of the EA maximum, but fitting is improved by assuming a hard-backed layer. The presence of a plough pan (hard layer) due to ploughing at depths of between 15 cm and 20 cm is well known but the disking process has a shallower effect [2].

5.5 Experiments and predictions involving roughness constructed from bricks

In a series of measurements deploying low parallel brick walls and brick lattices on car parks [44], a two-brick high rectangular lattice is found to offer a similar insertion loss to regularly-spaced parallel wall arrays of the same height but twice the total width. Part of the insertion loss due to the roughness configurations is the result of transfer of incident sound energy to surface waves which can be reduced by introducing wall absorption or material absorption in the form, for example, of shallow gravel layer between walls or in the lattice cells [25]. Predicted finite length effects are explored using a Pseudo-Spectral Time Domain Method, which models the complete 3D roughness profile. It is concluded from measurements and predictions that the lattice design has less dependence on azimuthal source-receiver angle than parallel wall configurations. These predictions are supported by the results of measurements of level difference spectra as a function of azimuthal angle.

The acoustical effects of parallel wall arrays can be predicted using a 2D BEM [25, 44]. Figure 14(b) compares such a prediction with laboratory data for the excess attenuation spectrum due to the arrangement in Figure 14(a).

Rather than having to carry out a BEM calculation with full discretisation of a parallel wall array, it is possible to predict the acoustical performance of low parallel wall arrays using a 2D BEM with the walls represented by raised effective impedance surfaces having an impedance given by the 2-parameter slit pore layer model [10, 25, 44]. This is illustrated by the comparison of predictions in Figure 15(b) for the arrangement shown in Figure 15(a).

Prediction of propagation over a lattice structure (see for example Figure 19(a)) is essentially a 3D problem. However a satisfactory raised impedance representation would allow use of a 2D prediction scheme. The accuracy of such a representation has been demonstrated through comparisons with laboratory data [25, 44].

Figure 16(a) is a vertical section schematic of a 0.2 m high brick lattice with a point source at a height of 0.1 m, and vertically-separated microphones at heights of 0.15 m and 0.05 m (above the lattice) at a horizontal separation of

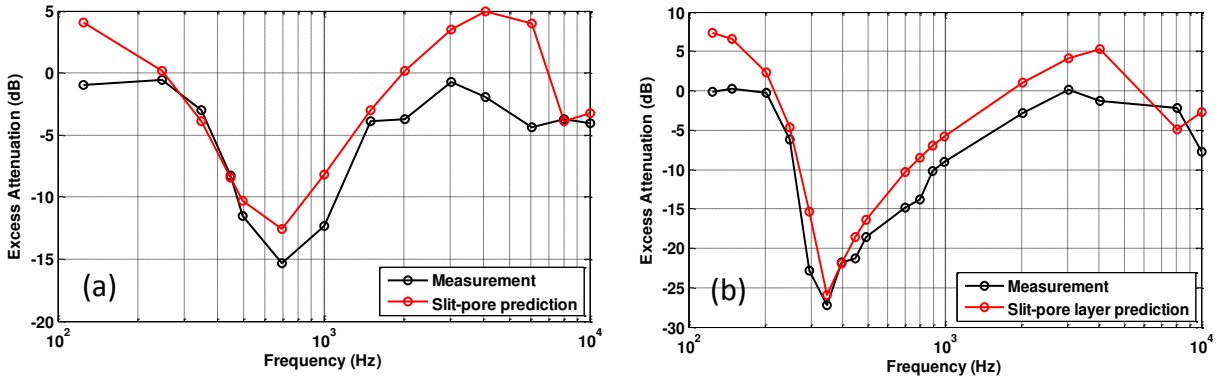

Figure 13: Comparisons between excess attenuation over weather-slaked fine sandy loam (data from Figure 3 of [38]; black joined circles) with source height = receiver height = 1.0 m, separation = 52.0 m (a) before disking and (b) after disking. Also shown are predictions (red joined circles) using a two parameter slit pore impedance model [10] (a) flow resistivity 270 kPa s m^{-2}, porosity 0.6) (b) flow resistivity 100 kPa s m^{-2}, porosity 0.7, layer depth 0.035 m.

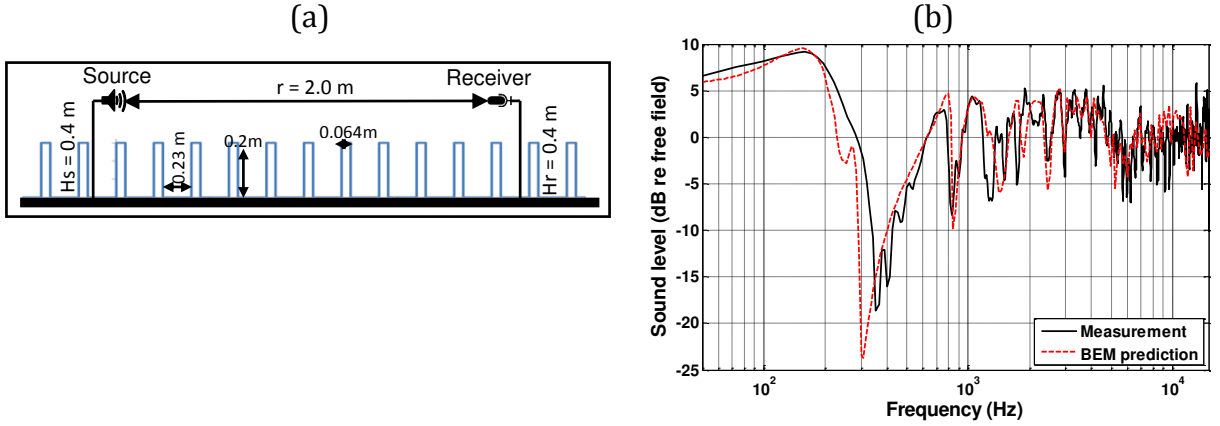

Figure 14: (a) Schematic of a laboratory arrangement with source and receiver at 0.4 m height over MDF with a separation of 2.0 m and over 0.2 m high and 0.064 m thick periodically spaced parallel brick walls placed in a 2.6 m wide array with centre-to-centre spacing of 0.28 m (b) comparison of measured EA spectrum with a BEM prediction made with full discretisation of the array.

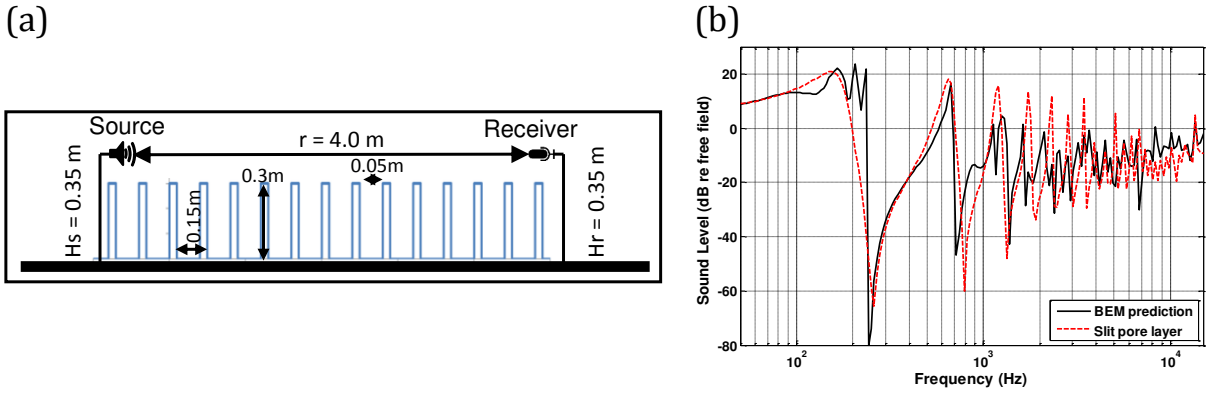

Figure 15: (a) Hypothetical array of 0.05 m thick and 0.3 m high parallel walls with centre-to-centre spacing of 0.2 m on an acoustically-hard surface with a line source and receiver at a height of 0.05 m above the tops of the parallel walls and a horizontal separation of 4.0 m (b) comparison of excess attenuation spectra predicted (i) using a 2D BEM with full discretisation of an array and (ii) for a point source over an impedance plane in which the top surface of the array is modelled as having a slit pore layer impedance deduced from the assumed wall geometry (flow resistivity = 0.0129 Pa s m^{-2}, porosity = 0.75 and layer depth = 0.3 m) [25].

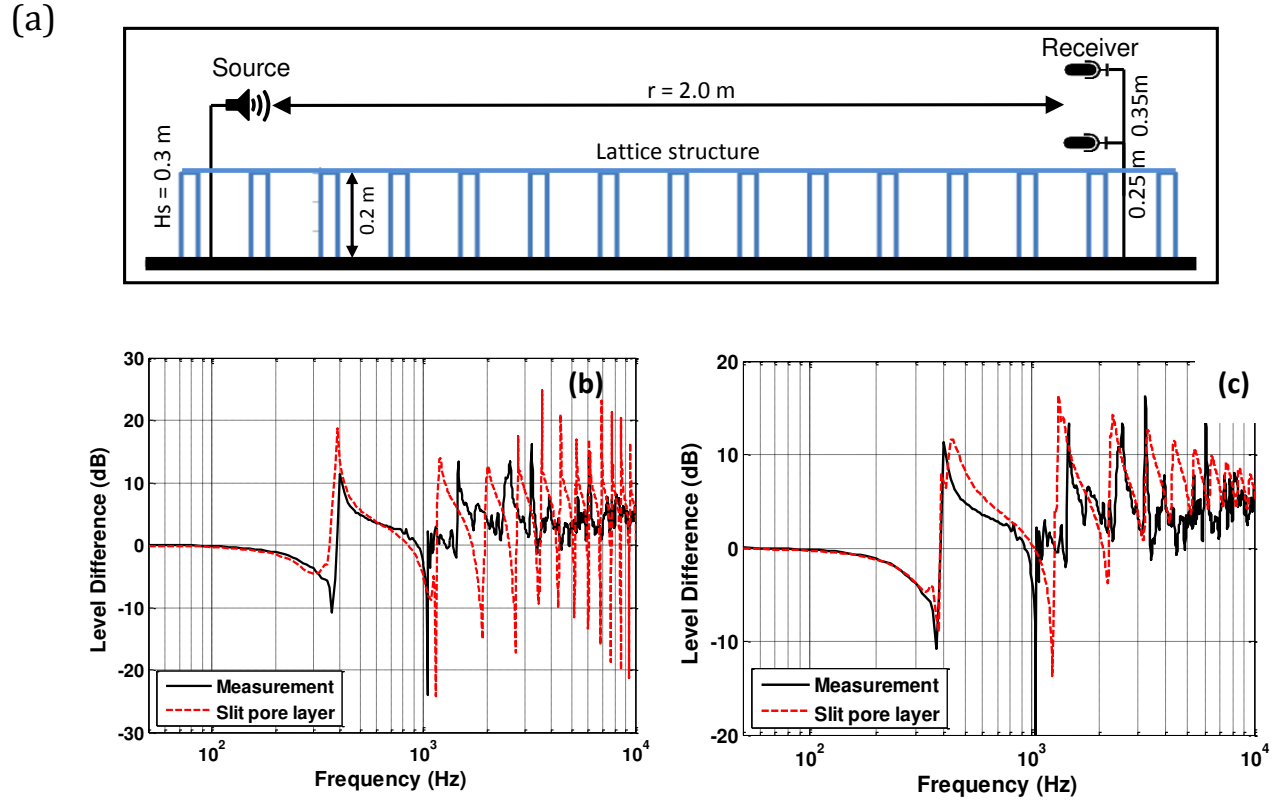

Figure 16: (a) Schematic vertical section showing vertically-separated microphones located at heights of 0.05 m and 0.15 m above a brick lattice from a (point) loudspeaker source placed at a height of 0.1 m above the lattice; (b) and (c) measured level difference spectra compared with BEM predictions in which the lattice is modelled as a raised impedance surface using a slit pore layer impedance model (b) with parameters based on the lattice geometry (flow resistivity = 0.04 Pa s m^{-2}. porosity = 0.54 and layer depth = 0.2 m) (c) with porosity 0.54 and adjusted values of effective flow resistivity (400 Pa s m^{-2}) and effective layer depth (0.16 m).

2.0 m from the source. Figure 16(b) compares a level difference spectrum measured over this arrangement outdoors with a prediction using a propagation model for a point source above an impedance plane with impedance predicted by the slit pore layer model. The impedance model parameters are deduced from the lattice geometry (flow resistivity = 0.04 Pa s m^{-2}. porosity = 0.54 and layer depth = 0.2 m). While there is good agreement between predictions and data below 1 kHz, at higher frequencies the amplitudes of the peaks and dips in the predicted level difference spectra differ appreciably from those in the measured level difference spectra. The discrepancies can be attributed to the effects of atmospheric turbulence (reducing coherence at high frequencies), air absorption and the fact that bricks are neither uniform nor acoustically hard. Figure 16(c) shows that improved agreement between predictions and data results from using effective parameters (effective flow resistivity 400 Pa s m^{-2} and effective layer depth 0.16 m) in the slit pore layer impedance model.

Data from horizontal level difference measurements made over a brick lattice on acoustically-hard asphalt using the geometry indicated in Fig. 17 are compared with 2D BEM predictions in which the lattice is modelled as a raised effective impedance surface in Figure 18 [25]. The loudspeaker source is placed at a height of 0.1 m and a distance of 2.0 m from one side of the lattice. A first microphone was placed 5.0 m from the source at a height of 0.25 m on the other side of the lattice and a second microphone was placed at a distance of 10 m from the source at heights of either 0.36 m or 0.85 m.

The rectangular form of the lattice used for outdoor measurements (see Figure 19(a)) [25, 44] has been found to give slightly different ground effects, represented by the level difference spectra shown in Figure 19(b), depending on the cell side length in the (orthogonal) axis of measurement [25]. The slightly larger cell dimension gives rise to a first level difference minimum (corresponding to an EA maximum) at a lower frequency. A similar dependence of excess attenuation spectra on the wall separation distance has been predicted for parallel wall arrays [25].

Figure 20 compares (fully-discretised) BEM numerical predictions and predictions using a semi-analytical

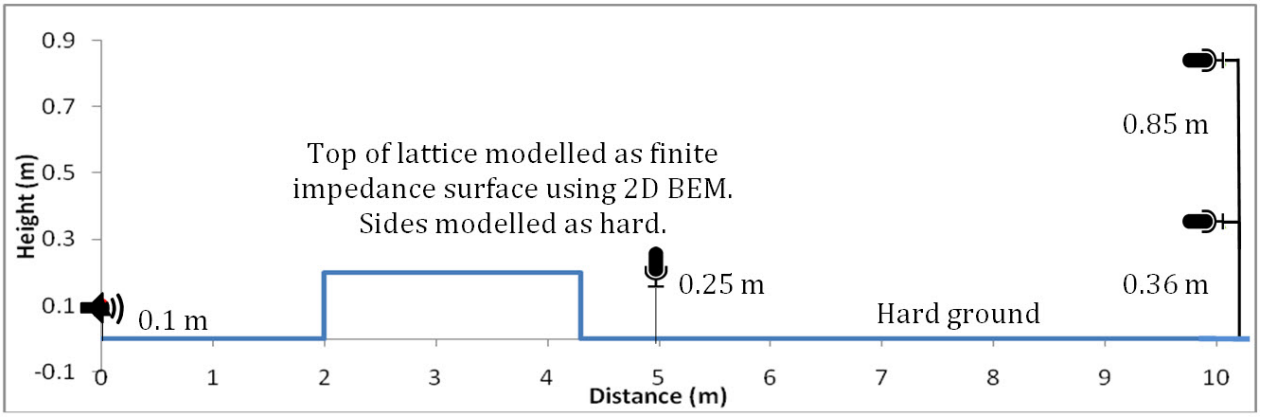

Figure 17: Schematic of horizontal level difference measurements and geometry assumed for predictions in which the lattice is modelled as a raised impedance surface.

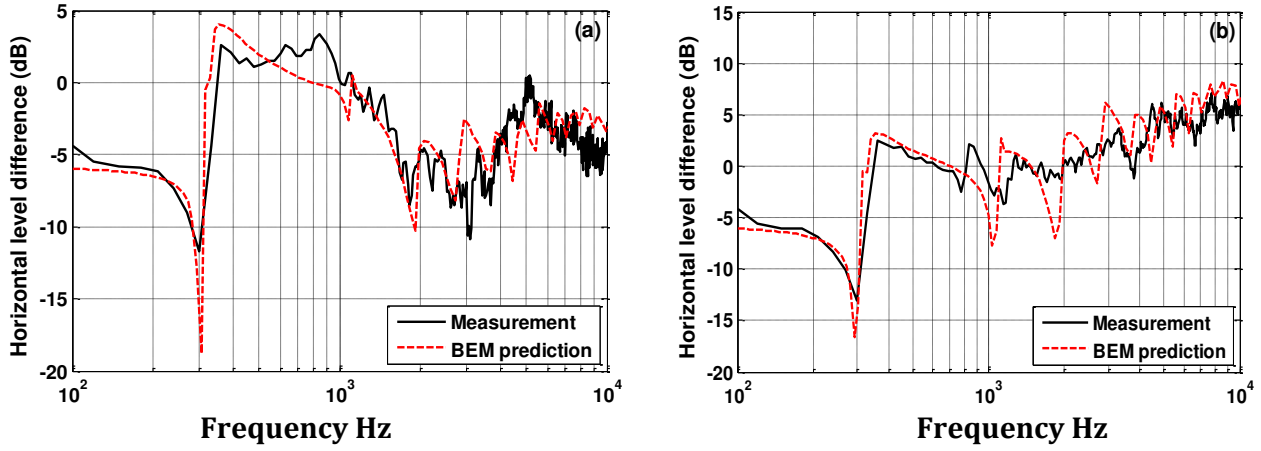

Figure 18: Level difference spectra measured over a brick Lattice with cell centre-to-centre spacing 0.28 m, height of 0.2 m and total width of 2.3 m using the geometry shown in Figure 15 with the second microphone at a height of (a) 0.36 m and (b) 0.85 m. Also shown are BEM predictions with the lattice modelled as the surface of a slit pore layer with flow resistivity = 400 Pa s m^{-2}, porosity = 0.55 and effective layer depth = 0.16 m.

method for a point source over a slit pore layer impedance, of the EA spectra due to a 0.3 m high parallel wall array in which each wall is 0.05 m thick. The source and receiver are assumed to be at a height of 0.05 m above the top of the wall array and separated by 4.0 m. The edge-to-edge spacings assumed are (a) 0.05 m and (b) 0.7 m. Again the frequency of the first EA maximum is predicted to decrease as the edge-to-edge spacing is increased. As shown by laboratory data [22, 34], the accuracy of predictions using the slit pore impedance model decreases with increasing edge-to-edge spacing. The slit pore layer impedance representation becomes inaccurate when the edge-to-edge separation exceeds the wall height.

6 Calculations of road noise reduction by ground treatment

Table 4 shows example predictions of the insertion losses due to various ground treatments at a 1.5 m and 4 m high receivers either 50 m or 100 m from the nearest edge of a two lane urban road containing 95% cars, 5% lorries travelling at 50 km/h. The point source arrays representing the vehicles are portrayed in Figure 21(a). The ground treatments starting at the edge of the road and receiver locations are shown schematically in Figures 21(b) to 21(e). To make the predictions, the HARMONOISE methodology for source characterisation [4] has been used. This assumes source heights of 0.01 m for road/tyre noise (all vehicles) and either 0.3 m (light and medium vehicles) or 0.75 m

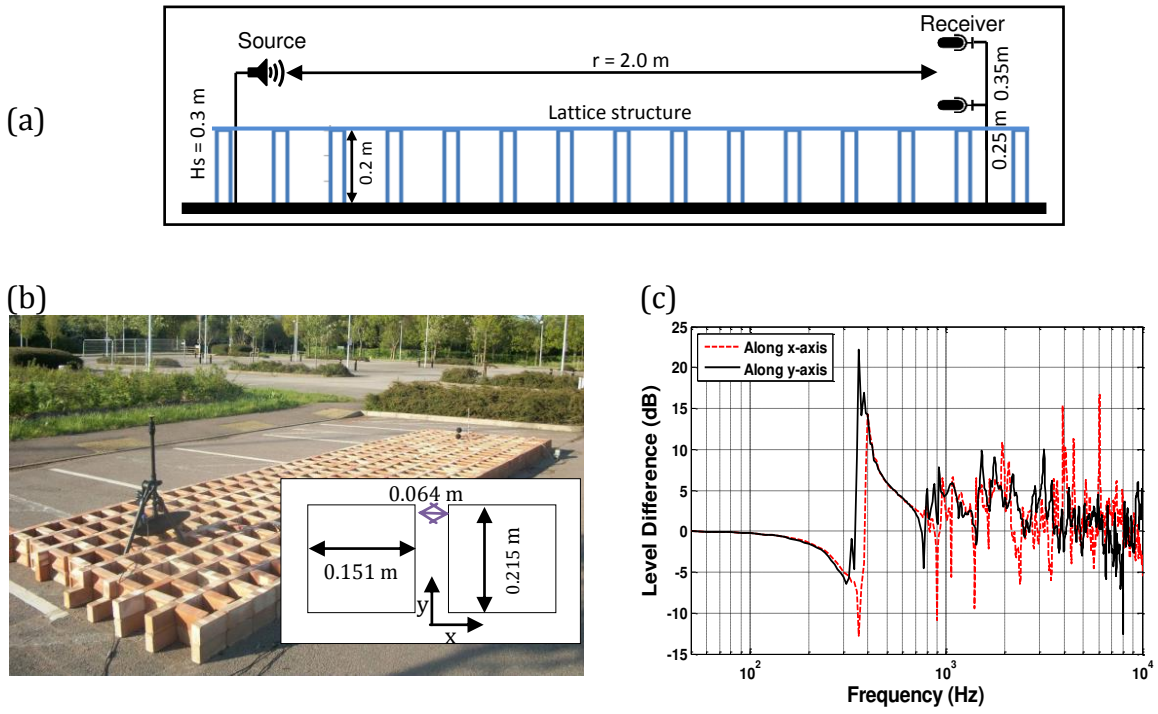

Figure 19: (a) and (b) Arrangement used for measuring the acoustical effects of a 0.2 m high rectangular brick lattice on a car park with source at height of 0.1 m, upper microphone at height of 0.15 m, lower microphone at height of 0.05 m and horizontal separation between them is of 2.0 m. ((c)) Comparison between measured level difference spectra measured along the "x-axis" and 'y-axis' of the lattice which correspond to the shorter and longer sides of the cells respectively.

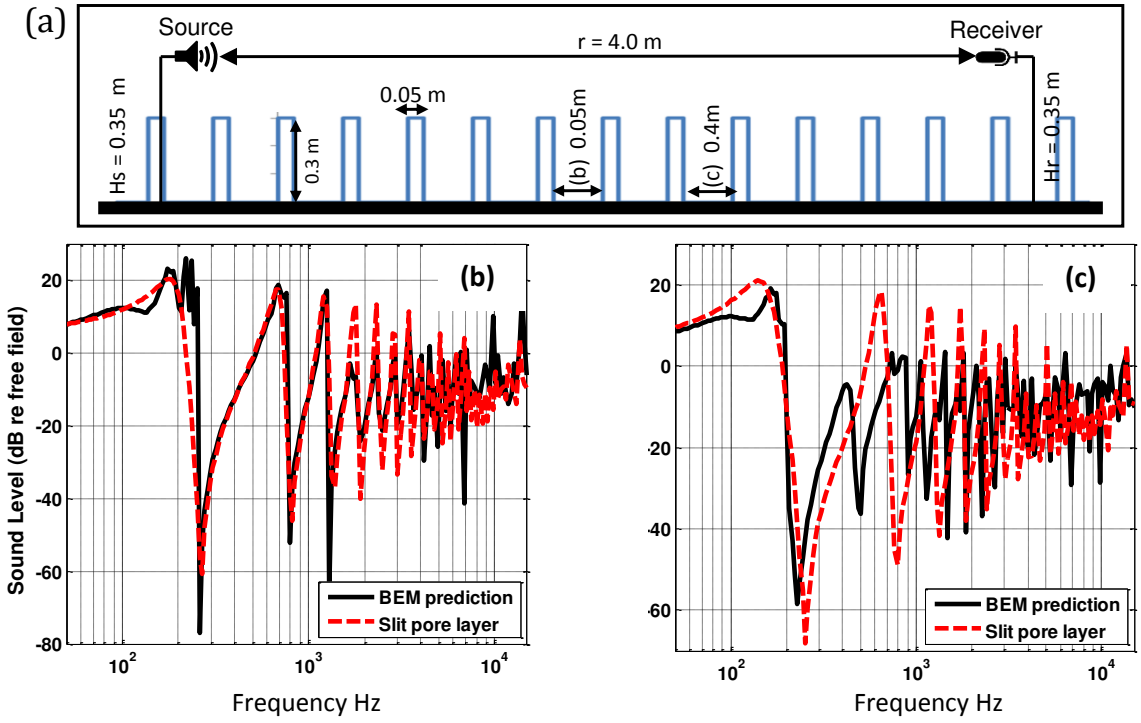

Figure 20: (a) Schematic showing source and receiver separated by 4.0 m and at a height of 0.05 m above the top of a 0.3 m high parallel wall array in which each wall is 0.05 m thick: (b) and (c) show EA spectra due to a 0.3 m high parallel wall array predicted using both BEM and a semi-analytical model for a point source over a slit pore layer impedance. The edge-to-edge spacings assumed are (b) 0.05 m and (c) 0.4 m which correspond to (b) flow resistivity 0.174 Pa s m^{-2}, porosity 0.5 and (c) flow resistivity 0.0015 Pa s m^{-2}, porosity 0.9.

Table 4: Insertion losses compared with smooth hard ground predicted for various parallel wall and lattice configurations for a receiver at a distance of 50 m or 100 m and at height of 1.5 m or 4 m. The ground treatments are assumed to start 2.5 m from the nearest traffic lane on a two-lane urban road (95% cars, 5% lorries travelling at 50 km/h) [25, 27, 44–46].

Receiver distance from road edge m	**50**		**100**	
height m	**1.5**	**4**	**1.5**	**4**
Ground treatment	**Insertion loss dB**			
Replacing a 47.5 m or 97.5 m wide strips of hard ground by high flow resistivity grassland	5.5	1.7	7.3	4.5
Replacing a 47.5 m or 97.5 m wide strip of hard ground by low flow resistivity grassland	7.6	2.0	12.1	6.3
Replacing a 50 m or 100 m wide strip of hard ground by low flow resistivity ground growing 1 m high dense crops	13.1	6.7	16.7	12.2
Replacing 25 m of hard ground nearest road by gravel (flow resistivity 10 kPa s m^{-2} at least 0.1 m deep)	9.1	3.0	9.3	7.5
Replacing 25 m of hard ground nearest road by alternating 1 m wide strips of hard ground and gravel (flow resistivity 10 kPa s m^{-2} at least 0.1 m deep)	7.3	2.8	6.9	6.3
1.65 m wide array of 9 parallel walls 0.3 m high, 0.05 m thick, 0.2 m centre-to-centre spacing	5.8	5.4	5.2	5.7
3.05 m wide array of 16 parallel walls, 0.05 m thick, 0.2 m centre-to-centre spacing	6.6	5.6	6.1	6.5
12.05 m wide array of 61 Parallel walls 0.3 m high, 0.05 m thick, 0.2 m centre-to-centre spacing	8.6	5.1	8.5	8.2
1.53 m wide 0.3 m high 0.2 m square cell lattice	5.9	5.6	5.3	5.8
3.05 m wide 0.3 m high 0.2 m square cell lattice	7.2	6.1	6.5	7.0
12.05 m wide 0.3 m high 0.2 m square cell lattice	10.5	6.1	10.0	9.6

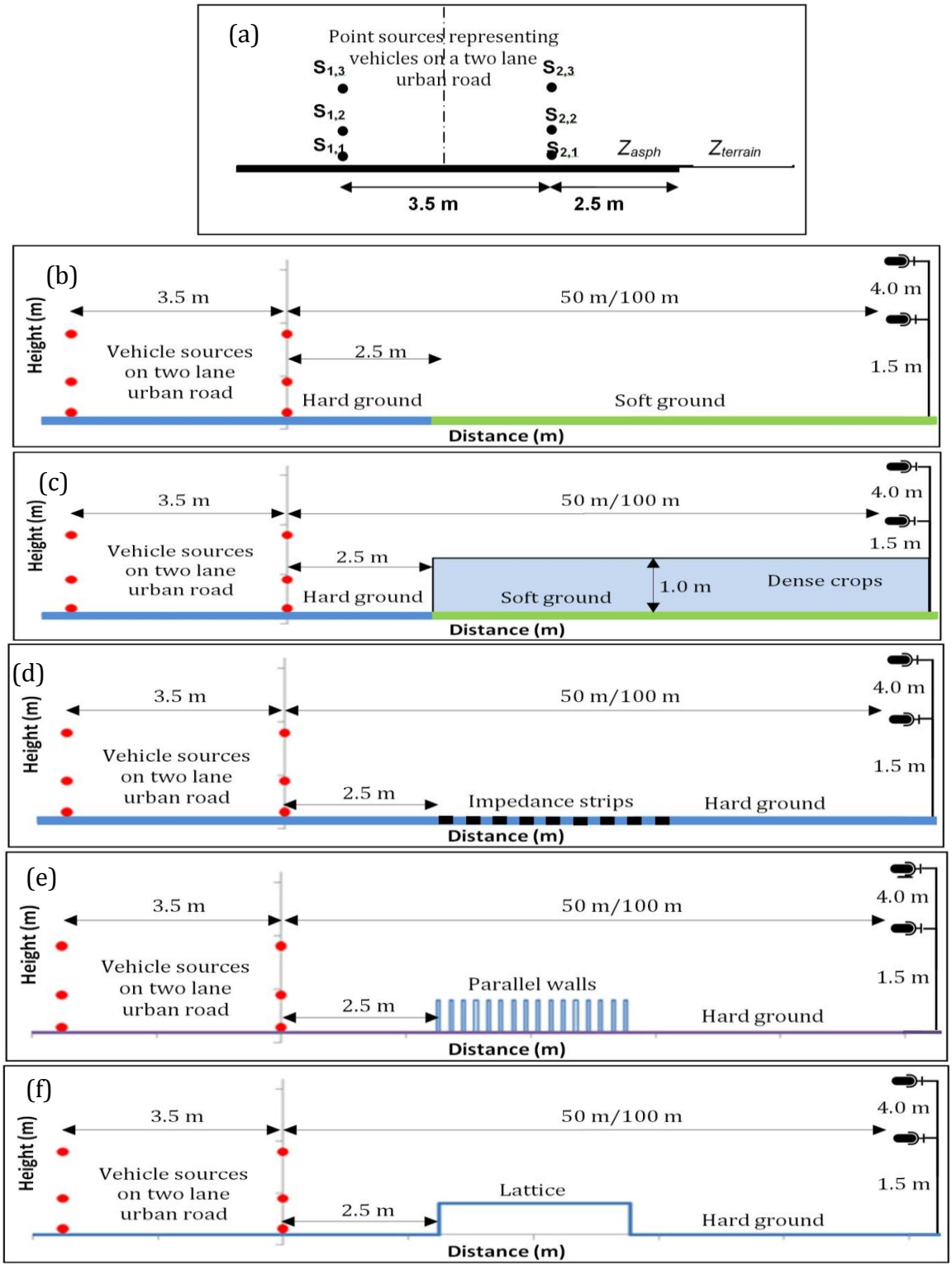

Figure 21: Schematic vertical sections of (a) two vertically-separated arrays of three point sources representing two lanes of vehicles on an urban road (b) soft ground treatment (c) soft ground with crops (d) 10 m or 25 m wide array of impedance strips (d) a 3 m wide 0.3 m high parallel low wall array and (e) a square lattice (of various widths). The receivers are either 1.5 or 4 m high and either 50 m or 100 m from the edge of the road.

Table 5: Reductions in overall levels due to the introduction of 100% "soft" ground next to a road predicted by Calculation of Road Traffic Noise (CRTN) [ref] and ISO9613-2.

width of soft ground from nearest road edge m	47.5		97.5	
Receiver height m	1.5	4.0	1.5	4.0
Prediction scheme	Reduction dB			
CRTN	5.5	3.3	7.0	4.8
ISO 9613-2	4.0	2.8	4.5	4.0

(heavy vehicles) for engine noise. The 1/3 octave spectrum of a vehicular noise source is specified by the vehicle type (*e.g.* car, LGV or HGV) and vehicle speed. A 2D BEM has been used to predict the *insertion losses* caused by ground treatments parallel to the road. For multiple lanes and a mix of vehicle types each source location is considered individually and the spectrum weighted according to the traffic flow percentage of each source. Multiple sources are treated as incoherent, *i.e.* the combination of two identical sources results in a 3 dB rather than a 6 dB increase. The predicted excess attenuation spectrum and distance attenuation correction is applied to each source and the contribution from each source summed at the receiver location. The insertion loss is calculated with respect to a smooth acoustically-hard surface, *i.e.* it is the difference in predicted levels before and after the ground treatment is introduced and takes account, therefore, of excess attenuation due to smooth hard ground. The treatments have been assumed to start 2.5 m from the nearest lane of vehicles *i.e.* at the edge of the road. Approximately 10 dB insertion loss is predicted by either replacing 47.5 m of hard ground with low flow resistivity soft ground or by constructing a 12 m wide array of 0.3 m high parallel walls on it.

The soft ground treatments are predicted to become less effective as the receiver height increases for a given distance from the source. For example the 5 to 10 dB insertion losses associated with replacing hard ground by soft ground using the example geometry shown in Figure 19 are reduced by about 5 dB at a 4 m high receiver.

The insertion losses predicted if hard ground is replaced by soft ground can be compared with those predicted by the Calculation of Road Traffic Noise (CRTN) scheme and by ISO9613-2 for comparable source-receiver geometries and are listed in Table 5.

As a result of replacing acoustically-hard by -soft ground, CRTN predicts comparable insertion losses to the more elaborate BEM predictions described despite the fact that CRTN assumes an effective source height of 0.5 m, *i.e.* higher than used in the other schemes, and, moreover, assumes a semi-lane width of 3.5 m rather than 2.5 m. Even with assuming the source height to be 0.05 m, ISO9613-2 predicts lower insertion losses for "soft" ground. However to make the ISO 9613-2 predictions the formula for predicting the reduction in A-weighted levels for broadband sources has been used rather than an octave band calculations. Neither CRTN or ISO 9613-2 predicts as great a dependence on receiver height as shown in Table 4. Also, as a result consequence of their limited consideration of ground effect, neither scheme predicts the potentially larger insertion losses (more than 5 dB greater for the 1.5 m high receiver and more than 1 dB higher for the 4 m high receiver) that are predicted in Table 4 for inserting lower flow resistivity surfaces, particularly those using gravel.

The predictions for a given receiver height listed in Table 4 indicate that, as the source-receiver distance is increased, the insertion losses due to near-source ground treatments do not decrease as they would with a traditional noise barrier. Indeed for some treatments they increase. This is because the effectiveness of ground treatments depends on the grazing angle of incidence from the source.

Parallel walls 0.3 m high in arrays at least 1.65 m wide are predicted to give comparable or higher insertion losses as predicted for continuous "soft" ground between the road edge and receivers 47.5 m or 97.5 m away and 1.5 m or 4 m high. Lattice configurations are predicted to give higher insertion losses than parallel wall arrays of the same width and height. Another advantage of a lattice configuration is that its efficacy is less dependent on the azimuthal source-receiver angle than that of a parallel wall array with the same height and width. It should be noted that, in contrast to the insertion loss due to "soft" ground, the insertion losses predicted for the lattice and parallel wall configurations are not much affected if the receiver height is increased from 1.5 m to 4 m. This is a consequence of the predicted insertion loss "beam" shown in Figure 22 which is a contour plot of overall insertion loss for a frequency range 178 Hz to 4.44 kHz due to a 0.2 m high 6 m wide lattice with 0.065 m thick walls and centre-to-centre spacing of 0.26 m starting 2.5 m from a 0.05 m high line source emitting a spectrum corresponding to 70 km/h light vehicular traffic. A "beam" of higher insertion loss compared with hard smooth ground (approximately 6 dB) extends from 0.2 m near the source to about 5 m height at 100 m. The slightly lower insertion loss (5 dB) predicted near the ground is a consequence of the roughness-induced surface wave. For motorways, calculations show that an increase of between 1 and 2 dB in the insertion loss would follow from deploying a 2 m wide 0.3 m high parallel wall or lattice configuration in the central

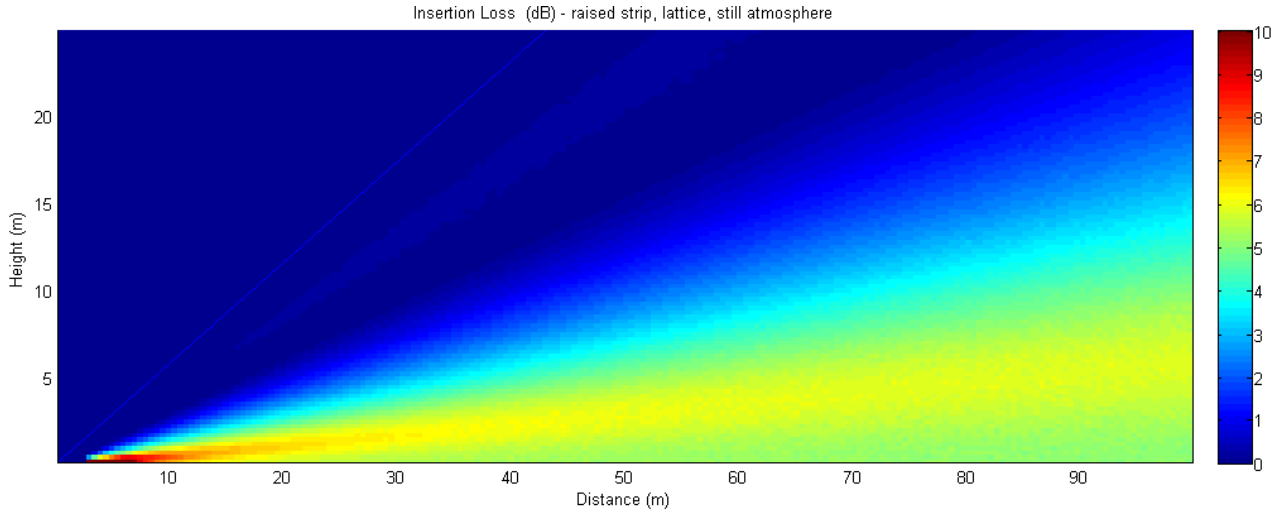

Figure 22: A plot of overall insertion loss contours from a 0.05 m high line source emitting a spectrum corresponding to light vehicles travelling at 70 km/h due to a 0.2 m high 6 m wide lattice.Numerical comparisons between the acoustical performances of raised lattices and those of equivalent recessed systems having identical "roughness" dimensions show that, typically a raised configuration insertion loss is predicted to be between 3 and 4 dB(A) higher than that for the equivalent recessed one [44, 46].

Table 6: Predicted insertion losses for a receiver at 1.5 m height and 50 m from a single lane of combined (5% heavy) road traffic sources moving at 70 km/h due to 8, 16 and 30 parallel wall arrays and due to either a single barrier corresponding to the nearest array wall or a single "thick" barrier of the same height and width as the arrays.

Number of walls (array width m)	8 (1.45 m)		16 (3.05 m)		30 (5.85 m)	
configuration	array	single	array	single	array	single
Insertion loss (dB)	8.8	5.7	10.2	5.9	11.3	6.2

reservation as well as along the side of the road [25, 46]. Although there is some effect due to the cross sectional shape of the roughness elements, the increase in noise reduction predicted, for example, when using equilateral triangular wedges rather than 0.3 m high rectangular wall cross sections (with the same cross sectional area) alongside a motorway is less than 1 dB [25, 46].

The predicted noise reduction due to the proposed ground treatments are lower if the proportion of heavy vehicles (which have higher engine noise sources than cars) is greater and if there are traffic lanes further from the treatment. For example at 47.5 m from the edge of a four lane motorway carrying 85% cars and 15% of lorries at a speed of 70 km/h a 15 m wide roughness array containing 26 parallel walls with equilateral triangular cross sections 0.247 m high starting 1 m from the nearside road edge is predicted to give noise reductions of 8.3 dB and 3.2 dB for receivers at heights of 1.5 m and 4 m respectively [25, 46].

The nearest element to the road in a 0.3 m high parallel wall array or lattice will act as a conventional barrier for the road/tyre source and to some extent for the 0.3 m high engine source. Consequently it is of interest to compare the predicted insertion loss due to a single thick 0.3 m high wall with that predicted for a parallel wall array of the same height and width. Figure 23 compares the predicted insertion loss spectra due to 0.3 m high and 3.05 m wide single "thick" and 16 multiple walls array with centre-to-centre spacing of 0.2 m and height of 0.3 m. The multiple edge diffraction and periodicity effects in the parallel walls introduce more attenuation than a single thick barrier. On the other hand, the multiple walls generate a surface wave. However all surfaces are assumed to be acoustically-hard in these calculations and the surface wave contributions are rapidly reduced by the introduction of absorption [25, 46].

Table 6 compares the insertion loss predicted at a receiver at 1.5 m height and 50 m from a single lane of combined ("engine" and "tyre/road") car sources moving at 70 km/h [19] due to 8, 16 and 30 parallel low wall systems with those predicted for a 'thick' barrier with the same height and width as the array "envelope". As a result of the physical mechanisms discussed, arrays of low parallel thin walls are predicted to offer a significantly higher insertion loss than a single thick low wall. The difference in

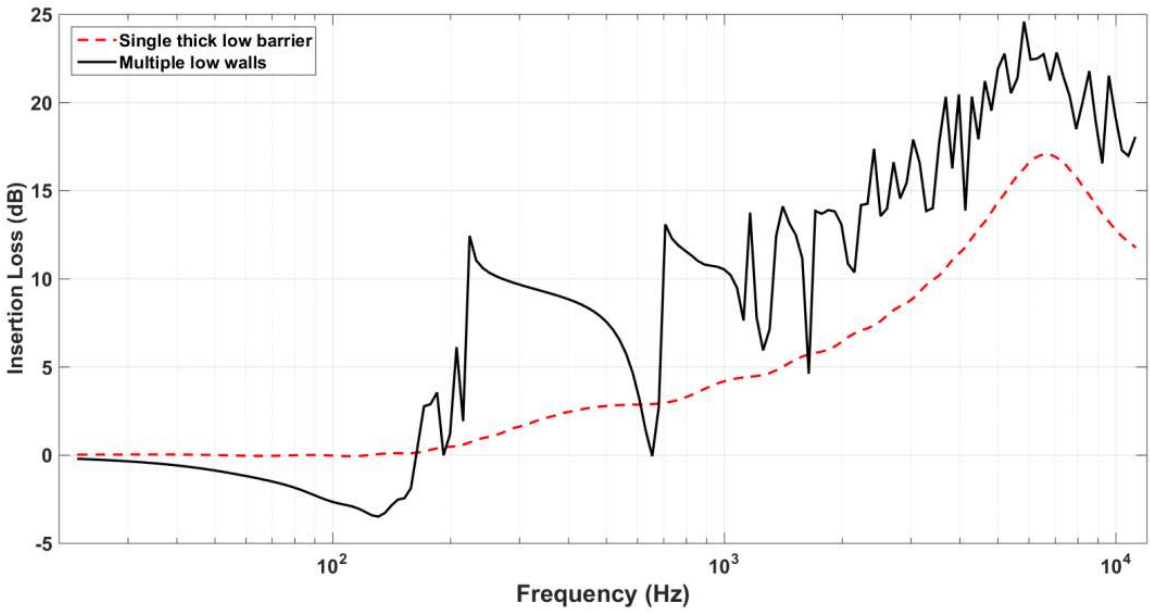

Figure 23: Comparison between excess attenuation spectra for a 0.01 m high source and 1.5 m high receiver predicted for a single 0.3 m high 3.05 m wide barrier and for a 16 × 0.05 m thick 0.3 m high 3.05 m wide array of parallel walls with 0.2 m centre-to-centre spacing. The distance between the source and receiver is assumed to be 50 m.

overall insertion loss is greatest (5.1 dB) for a 30 × 0.3 m high 5.85 m wide wall array which is predicted to offer an insertion loss of 11.3 dB for the single lane of combined traffic sources and a 1.5 m high receiver 50 m away. To obtain a similar overall insertion loss a single thin wall (0.05 m wide) at the nearest wall location would have to be 0.75 m high.

7 Discussion

Ground effects can be exploited for noise control. Even though it is difficult to achieve as much reduction as might be obtained with a traditional noise barrier of, say, 1 m height, the advantage of exploiting ground effect is that it does not create an impassable division between communities. Also replacing acoustically-hard ground by acoustically-soft ground offers the opportunity of adding to the "green" in cities. To some extent, the possibility of using soft ground for noise abatement could follow from use of the full range of (effective) flow resistivity values specified by the CNOSSOS-EU scheme [3]. A calculation for 1.5 m high receiver in the road traffic noise geometry shown in Figure 19 using the lowest listed grassland flow resistivity (80 kPa s m^{-2}) in Table 1 and assuming the (physically inadmissible) single parameter impedance model, predicts an insertion loss due to replacing hard ground by soft ground of 8.9 dB *i.e.* slightly less than the 10.5 dB predicted by using a physically admissible impedance model. A smaller insertion loss of about 5 dB is associated with using the highest flow resistivity value for soft ground listed in Table 1 (500 kPa s m^{-2}) for the 1.5 m receiver in the geometry in Figure 19.

Moreover the ground type descriptions in Table 1 contain the clue that the most effective type of soft ground is uncompacted. Table 4 shows also that soft ground effects can be augmented in an acoustically-beneficial way (for further noise reductions of between 2 and 5 dB) by 1 m high dense crops (or other dense vegetation) [27, 44, 46]. The planting of crops can have a longer influence on ground effect than the seasonal effect of the vegetation as a result of creating root zones. Ground compaction can be avoided both by growing vegetation and by avoiding use of heavy machinery during cultivation.

The scheme in Directive 2015/996 [3] does not consider the effects of vegetation or small scale roughness. Significant reductions in surface transport noise (up to 10 dB) can be obtained by the deliberate introduction of an at least 3 m wide strip of 0.3 m high roughness on flat hard ground. A particularly effective form of roughness has the form of a 0.3 m high 0.2 m side 3 m wide square cell lattice which offers greater insertion loss and has less azimuthal angle dependence than a parallel wall array with 0.2 m spacing and 3 m width. Since the cells in the proposed lattice structures are significantly larger than the

pores in porous asphalt they will not become clogged. Nevertheless to prevent accumulation of detritus they could be protected by acoustically-transparent meshes or indeed be used for planting without reducing their performance substantially. Roughness treatments can be recessed but this reduces their insertion loss by about 3 dB. On the other hand even though recessed systems are predicted to be acoustically less effective and, potentially, they are more expensive to construct, they might be preferred where there are restrictions on above ground constructions close to roads or where they might be combined usefully with drainage arrangements. It would be possible to recover some of the reduced insertion loss by starting them closer to the noise source or by making the recessed configurations deeper than 0.3 m. Placing a roughness-based noise reducing arrangement nearer to the source will make it less susceptible to the meteorological effects mentioned later.

Although ground-roughness-based reductions are comparable only with those offered by a relatively low (0.75 m high) single barrier and use more land, they might be an attractive alternative to such a barrier where it is desirable to preserve line of sight. Indeed, unlike the traditional barrier, the acoustical performance of a roughness treatment is not reduced significantly if a path is made through it [25]. Also unlike a conventional noise barrier, the acoustical performance of some near-source ground treatments increase as the source-receiver distance is increased. However, in common with a conventional noise barrier, the insertion loss of a ground treatment is reduced by downward refracting and turbulent meteorological conditions.

A cost benefit analysis of the deployment of lattices alongside and in the central reservation of a four lane road suggests that they could be a useful alternative to traditional noise barriers particularly when used in combination with low noise road surfaces [46]. There are similar possibilities for exploiting ground effects to reduce railway and tram noise and discussion of these can be found elsewhere [25, 45, 46].

Acknowledgement: The research leading to these results has received funding from the European Community's Seventh Framework Programme (FP7/2007-2013) under grant agreement n° 234306, collaborative project HOSANNA. We are grateful also for the comments from two anonymous reviewers that have helped to improve the paper.

References

[1] ISO, Acoustics–Attenuation of Sound During Propagation Outdoors–Part 2: A General Method of Calculation (ISO 9613-2). (ISO, Geneva, Switzerland, 1996)

[2] K. Attenborough, K. M. Li, K. Horoshenkov, Predicting Outdoor Sound, Taylor and Francis, London, 2007

[3] Annex to Commission Directive 2015/996 in Official Journal of the European Union L168 (2015)

[4] R. Nota, R. Barelds, D. Van Maercke, Harmonoise WP 3 Engineering method for road traffic and railway noise after validation and fine tuning, Deliverable of WP3 of the HARMONOISE project. Document ID HAR32TR-040922-DGMR20, 2005

[5] NORD2000. Comprehensive outdoor sound propagation model. Part 1. Propagation in an atmosphere without significant refraction. Report AV 1849/00 Delta Acoustics http://www.madebydelta.com/imported/images/DELTA_Web/documents/TC/acoustics/Nord2000/av185100rev_Nord2000_Propagation_Model2.pdf (date last viewed 11/01/16) (2006)

[6] S. Taherzadeh, K. Attenborough, Deduction of ground impedance from measurements of excess attenuation spectra. J. Acoust. Soc. Am. 1999, 105 2039–2042

[7] ANSI/ASA S1.18-2010. American National Standard Method for Determining the Acoustic Impedance of Ground Surfaces (revision of S1.18-1998)

[8] NORDTEST ACOU 104. Ground Surfaces: determination of acoustic impedance, 1998. http://doutoramento.schiu.com/referencias/outras/NT%20ACOU%2014%20-%20Ground%20Surfaces%20Determination%20of%20acoustic%20impedance.%20199 9.pdf (date last viewed 2/01/16)

[9] M. Delany, E. N. Bazley, Acoustical properties of fibrous absorbent materials, Appl. Acoust. 1970, 3, 105–116

[10] K. Attenborough, I. Bashir, S. Taherzadeh, Outdoor ground impedance models, J. Acoust. Soc. Am. 2011, 129, 2806–2819

[11] D. Dragna, K. Attenborough, P. Blanc-Benon, On the inadvisability of using single parameter models for representing the acoustical properties of ground surfaces, J. Acoust. Soc. Am. 2015, 138, 2399–2413, dx.doi.org/10.1121/1.4931447

[12] H. Taraldsen, G. Jonasson, Aspects of ground effect modeling, J. Acoust. Soc. Am. 2011, 129, 47–53

[13] D. Dragna, P. Blanc-Benon, Physically admissible impedance models for time-domain computations of outdoor sound propagation, Acta Acust. united Ac. 2014, 100, 401–410

[14] Road noise prediction,2 -Noise propagation computation method including meteorological effects (NMPB 2008), SETRA (2009) downloaded from http://www.setra.developpement-durable.gouv.fr/ (last viewed 02/01/16)

[15] G. Guillaume, F. Faure, B. Gauvreau, F. Junker, M. Berengier, Estimation of impedance model input parameter from in situ measurements: Principles and applications, Appl. Acoust. 2015, 95, 27–36

[16] J. S. Robertson, P. J. Schlatter, W. L. Siegmann, Sound propagation over impedance discontinuities with the parabolic approximation, J. Acoust. Soc. Am. 1996, 99, 761–767

[17] D. C. Hothersall, J. N. B. Harriott, Approximate models for sound propagation above multi-impedance plane boundaries, J. Acoust. Soc. Am. 1995, 97, 918–926

[18] K. B. Rasmussen, Propagation of road traffic noise over level terrain, J. Sound Vib. 1982, 82, 51–61

[19] M. Naghieh, S. I. Hayek, Diffraction of a point source by two impedance covered half-planes, J. Acoust. Soc. Am. 1981, 69, 629–637

[20] B. O. Enflo, P. H. Enflo, Sound wave propagation from a point source over a homogeneous surface and over a surface with an impedance discontinuity, J. Acoust. Soc. Am. 1987, 82, 2123–2134

[21] B. A. de Jong, A. Moerkerken, J. D. van der Toorn, Propagation of sound over grassland and over an earth barrier, Journal of Sound and Vibration 1983, 86, 23–46

[22] G. A. Daigle, J. Nicolas, J. L. Berry, Propagation of noise above ground having an impedance discontinuity, J. Acoust. Soc. Am. 1985, 77, 127–138

[23] P. Boulanger, T. Waters-Fuller, K. Attenborough, K. M. Li, Models and measurements of sound propagation from a point source over mixed impedance ground, J. Acoust. Soc. Am. 1997, 102, 1432–1442

[24] Y. W. Lam, M. R. Monazzam, On the modeling of sound propagation over multi-impedance discontinuities using a semiempirical diffraction formulation, J. Acoust. Soc. Am. 2006, 120, 686–698

[25] I. Bashir, Acoustical exploitation of rough, mixed impedance and porous surfaces outdoors, PhD Thesis, Engineering and Innovation, The Open University, 2014

[26] (a) D. Aylor, Noise reduction by vegetation and ground, J. Acoust. Soc. Am. 1972, 51, 197–205 (b) D. Aylor, Sound Transmission through Vegetation in Relation to Leaf Area Density, Leaf Width, and Breadth of Canopy, J. Acoust. Soc. Am. 1972, 51, 411–418

[27] I. Bashir, S. Taherzadeh, H.-C. Shin, K. Attenborough, Sound propagation over soft ground with and without crops and potential for surface transport noise reduction, J. Acoust. Soc. Am. 2015, 137, 154–164, http://dx.doi.org/10.1121/1.4904502

[28] P. Boulanger, K. Attenborough, S. Taherzadeh, T. Waters-Fuller, K. M. Li, Ground Effect Over Hard Rough Surfaces, J. Acoust. Soc. Am. 1998, 104, 1474–1482

[29] K. Attenborough, T. Waters-Fuller, Effective impedance of rough porous ground surfaces, J. Acoust. Soc. Am. 2000, 108, 949–956

[30] J. P. Chambers, J. M. Sabatier, R. Raspet, Grazing incidence propagation over a soft rough surface, J. Acoust. Soc. Am. 1997, 102, 55–59

[31] A. Whelan, J. P. Chambers, A note on the effects of roughness on acoustic propagation past curved rough surfaces, J. Acoust. Soc. Am. 2009, 125, EL231–EL235

[32] P. Boulanger, K. Attenborough, Q. Qin, Effective impedance of surfaces with porous roughness: Models and data, J. Acoustic. Soc. Am. 2004, 117, 1146–1156

[33] I. Tolstoy, Coherent sound scatter from a rough interface between arbitrary fluids with particular reference to roughness element shapes and corrugated surfaces, J. Acoust. Soc. Am. 1982, 72, 960–972

[34] I. Tolstoy, Smoothed boundary conditions, coherent low-frequency scatter, and boundary modes, J. Acoust. Soc. Am. 1983, 72, 1–22

[35] R. J. Lucas, V. Twersky, Coherent response to a point source irradiating a rough plane, J. Acoust. Soc. Am. 1984, 76, 1847–1863

[36] L. A. M. van der Heijden, M. J. M Martens, Traffic noise reduction by means of surface wave exclusion above parallel grooves in the roadside, Applied Acoustics 1982, 15, 329–339

[37] H. Bougdah, I. Ekici, J. Kang, A laboratory investigation of noise reduction by rib-like structures on the ground, J. Acoust. Soc. Am. 2006, 120, 3714–3722

[38] I. Bashir, S. Taherzadeh, K. Attenborough, Diffraction-assisted rough ground effect: models and data, J. Acoust. Soc. Am. 2013, 133, 1281–1292

[39] I. Bashir, S. Taherzadeh, K. Attenborough, Surface waves over periodically spaced strips, J. Acoust. Soc. Am. 2013, 134, 4691–4697

[40] G. A. Daigle, M. R. Stinson, D. I. Havelock, Experiments on surface waves over a model impedance plane using acoustical pulses, J. Acoust. Soc. Am. 1996, 99, 1993–2005

[41] W. Zhu, M. Stinson, G. A. Daigle, Scattering from impedance gratings and surface wave formation, J. Acoust. Soc. Am. 2002, 111, 1996–2012

[42] W. Zhu, G. A. Daigle, M. Stinson, Experimental and numerical study of air-coupled surface waves generated above strips of finite impedance, J. Acoust. Soc. Am. 2003, 114, 1243–1253

[43] J. P. Chambers, J. M. Sabatier, Recent advances in utilizing acoustics to study surface roughness in agricultural surfaces, Applied Acoustics 2002, 63, 795–812

[44] S. Taherzadeh, I. Bashir, T. Hill, K. Attenborough, M. Hornikx, Reduction of surface transport noise by ground roughness, Applied Acoustics 2014, 83, 1–15, DOI: 10.1016/j.apacoust.2014.03.011

[45] T van Renterghem, J Forssen, K Attenborough, P Jean, J Defrance, M Hornikx, J Kang, Using natural means to reduce surface transport noise during propagation outdoors, Applied Acoustics 2015, 92, 86–101, DOI: 10.1016/j.apacoust.2015.01.004

[46] Environmental Methods for Transport Noise Reduction ed Nilsson *et al.*, Cat/ISBN: Y119572 / 9780415675239 CRC Press an imprint of Taylor and Francis New York, 2014